1996-12

Evaluation of low altitude rocket dropsondes for shipboard atmospheric profiling and electromagnetic propagation assessment

Baldauf, Brian Keith

Monterey, California. Naval Postgraduate School

NAVAL POSTGRADUATE SCHOOL
MONTEREY, CALIFORNIA

THESIS

EVALUATION OF LOW ALTITUDE ROCKET DROPSONDES FOR SHIPBOARD ATMOSPHERIC PROFILING AND ELECTROMAGNETIC PROPAGATION ASSESSMENT

by

Brian Keith Baldauf

December, 1996

Thesis Co-Advisors: Kenneth L. Davidson
Carlyle H. Wash

Approved for public release; distribution is unlimited.

REPORT DOCUMENTATION PAGE

Form Approved OMB No. 0704-0188

1. AGENCY USE ONLY *(Leave blank)*	2. REPORT DATE	3. REPORT TYPE AND DATES COVERED
	December, 1996	Master's Thesis

4. TITLE AND SUBTITLE
EVALUATION OF LOW ALTITUDE ROCKET DROPSONDES FOR SHIPBOARD ATMOSPHERIC PROFILING AND ELECTROMAGNETIC PROPAGATION ASSESSMENT

5. FUNDING NUMBERS

6. AUTHOR(S) Brian Keith Baldauf

7. PERFORMING ORGANIZATION NAME(S) AND ADDRESS(ES)
Naval Postgraduate School
Monterey CA 93943-5000

8. PERFORMING ORGANIZATION REPORT NUMBER

9. SPONSORING/MONITORING AGENCY NAME(S) AND ADDRESS(ES)

10. SPONSORING/MONITORING AGENCY REPORT NUMBER

11. SUPPLEMENTARY NOTES The views expressed in this thesis are those of the author and do not reflect the official policy or position of the Department of Defense or the U.S. Government.

12a. DISTRIBUTION/AVAILABILITY STATEMENT
Approved for public release; distribution is unlimited.

12b. DISTRIBUTION CODE

13. ABSTRACT *(maximum 200 words)*

A study was performed on two measurement systems used to obtain profiles of refraction from a ship; the radiosonde and the rocketsonde. Refractive conditions measured by the Marwin Rawinsonde Set (MRS) utilizing radiosondes launched from U.S. Navy ships can yield misleading modified refractivity (M) versus height profiles. MRS obtained M unit profiles, when incorporated in propagation loss models such as Radio Physical Optics (RPO), also may produce unrepresentative propagation loss assessments. Rocketsonde obtained environmental parameters (temperature, relative humidity, pressure) are measured away from the ships influence. The ship can modify the environmental parameters and affect temperatures by as much as 3° C. Rocketsonde obtained data yield improved fine-scale vertical resolution. Resolution approaching 5m obtained via rocketsondes is found to most closely resemble the actual environment. Rocketsonde data is available down to the near-surface whereas there is a distinct lack of data from the surface to the launch point when utilizing balloon launched radiosondes. Inaccuracies in initial surface data drastically impact refractive profiles. Rocketsondes can be used regardless of sea state or wind conditions onboard ship and require no specific ship mancuvering to safely launch. It is found that the rocketsonde can obtain the requisite environmental parameters for refractive assessment on demand in less than half the time required to prepare and launch a balloon guided radiosonde.

14. SUBJECT TERMS Environmental Data, Radio Physical Optics, Radar Performance Prediction, Radiosonde, Refraction, Rocketsonde, SHAREM 110, Surface Based Duct			15. NUMBER OF PAGES 158
			16. PRICE CODE
17. SECURITY CLASSIFICATION OF REPORT Unclassified	18. SECURITY CLASSIFICATION OF THIS PAGE Unclassified	19. SECURITY CLASSIFICATION OF ABSTRACT Unclassified	20. LIMITATION OF ABSTRACT UL

NSN 7540-01-280-5500

Standard Form 298 (Rev. 2-89)
Prescribed by ANSI Std. 239-18 298-102

Approved for public release; distribution is unlimited.

EVALUATION OF LOW ALTITUDE ROCKET DROPSONDES FOR SHIPBOARD ATMOSPHERIC PROFILING AND ELECTROMAGNETIC PROPAGATION ASSESSMENT

Brian Keith Baldauf
Lieutenant Commander, United States Navy
B.S., University of Delaware, 1985

Submitted in partial fulfillment
of the requirements for the degree of

MASTER OF SCIENCE IN METEOROLOGY AND PHYSICAL OCEANOGRAPHY

from the

NAVAL POSTGRADUATE SCHOOL
December 1996

ABSTRACT

A study was performed on two measurement systems used to obtain profiles of refraction from a ship; the radiosonde and the rocketsonde. Refractive conditions measured by the Marwin Rawinsonde Set (MRS) utilizing radiosondes launched from U.S. Navy ships can yield misleading modified refractivity (M) versus height profiles. MRS obtained M unit profiles, when incorporated in propagation loss models such as Radio Physical Optics (RPO), also may produce unrepresentative propagation loss assessments. Rocketsonde obtained environmental parameters (temperature, relative humidity, pressure) are measured away from the ships influence. The ship can modify the environmental parameters and affect temperatures by as much as 3° C. Rocketsonde obtained data yield improved fine-scale vertical resolution. Resolution approaching 5m obtained via rocketsondes is found to most closely resemble the actual environment. Rocketsonde data is available down to the near-surface whereas there is a distinct lack of data from the surface to the launch point when utilizing balloon launched radiosondes. Inaccuracies in initial surface data drastically impact refractive profiles. Rocketsondes can be used regardless of sea state or wind conditions onboard ship and require no specific ship maneuvering to safely launch. It is found that the rocketsonde can obtain the requisite environmental

parameters for refractive assessment on demand in less than half the time required to prepare and launch a balloon guided radiosonde.

TABLE OF CONTENTS

I. INTRODUCTION

The sophisticated systems and tactics employed by today's Naval forces are extremely sensitive to variations in atmospheric parameters. In particular, electromagnetic (EM) sensors utilized to support Naval operations are designed to exploit specific propagation effects at specific wavelengths, and thus are extremely sensitive to variations in atmospheric parameters.

The two key components in providing accurate shipboard assessment of propagation conditions and sensor performance are the implementation of efficient, accurate, range-dependent models in conjunction with high vertical resolution atmospheric data. Successful and accurate propagation models utilizing the parabolic wave equation (PE) solved with a numerical technique such as the Fourier split-step are widely used and have proven to be in excellent agreement with measured propagation loss.

The focus has now been shifted to obtaining high vertical resolution atmospheric data. A weakness in propagation assessment is correlated with the manner in which environmental data is acquired. Current upper-air observing systems, such as the untethered balloon-guided radiosonde utilized by ship's at-sea, provide atmospheric data that may not have sufficient spatial and temporal resolution for propagation assessment in programs and tactical decision aids such as Tactical Environmental Support System (TESS) or Integrated Refractive Effects Prediction System (IREPS). The balloon-guided radiosonde may not accurately characterize the lower levels of the environment and when used in conjunction with assessment programs such as TESS or IREPS can provide an unrealistic description of low-level sensor performance. This weakness in data acquisition ultimately impacts the derived environmental

products and tactical decision aids supporting warfare requirements which directly impacts the effect of Naval operations. In terms of improving the end or derived product, one must look to improve the data resolution and accuracy.

To provide maximum prediction accuracy, fine-scale vertical profiles of temperature, pressure, and relative humidity must be made within the region for which propagation loss is to be calculated. These parameters are critical in determining atmospheric refractivity. Several technologies are emerging, including the Deck Launched Sonde (DELS) and the Tactical Dropsonde (TDROP), that support this concept, but they remain several years from becoming operationally tested and implemented. The Low Altitude Rocket Dropsonde System (LARDS) is a low-cost, effective, and readily available system that can be utilized onboard ships at-sea. It can provide fine-scale vertical resolution away from the ship's effluence delivering a better "snapshot" of representative atmospheric refractive conditions and ultimately a drastic improvement in propagation prediction accuracy. This low-cost disposable rocket carries a lightweight telemetry package to an altitude of 10,000 ft. The instrument package is ejected from the rocket and is parachuted to the surface while telemetering to the ship the required fine-scale measurements of temperature, pressure, and relative humidity.

The low altitude rocket dropsonde provides three distinct advantages over the conventional balloon launched radiosonde. The rocket launched probe can be considered an all-weather instrument capable of providing atmospheric profiling data regardless of wind conditions or sea state. Secondly, balloon guided radiosondes launched from ships at-sea may be contaminated in the vicinity of the ship due to discharge of ship's effluence and large heat

signature as well as changes in the environment immediately surrounding the ship. Lastly, the ability to accurately characterize the EM propagation and assess the performance of surface-based surface search radars such as the U.S. Navy's SPS-10 requires measurements with a vertical resolution of a few meters (m) extending to the water surface. Although the near surface conditions are not necessarily well represented by a single measurement due to the dynamic variability of the low-level atmospheric structure produced by mixing processes, the rocketsonde does provide a representative picture of the near surface conditions at the time of measurement.

This thesis will concentrate on the analysis of recent simultaneously obtained rocketsonde and radiosonde data from operational U.S. Navy ships. Profiles depicting the refractive conditions from the radiosonde and rocketsonde data will be utilized for analysis. The issue becomes even more complex when considering the highly variable littoral regions. Rocketsonde and balloon launched radiosonde data collected from a recently conducted CNO sponsored exercise will be utilized in conjunction with data collected from the first-ever rocketsonde launch from a U.S. Navy aircraft carrier, USS Kitty Hawk (CV 63), to assess the need for a better means of characterizing the low altitude refractive profiles and radar performance predictions. The assessed refractive conditions will subsequently be used in a propagation loss model, Radio Physical Optics (RPO), to illustrate the significant variation in propagation loss. This variation in assessed propagation loss will be shown to directly impact the predicted range for a particular sensor of interest. This study will illustrate the need for a finer scale data resolution for shipboard derived environmental data that must be obtained away from the ship's influence.

II. BACKGROUND

A. PURPOSE

The major emphasis of Naval operations center on the projection of power ashore. Recently, the Naval mission has shifted from what has been termed "blue" or open ocean warfare to warfare concentrated in a more localized littoral regions. This new emphasis is composed of two distinct battle spaces. The seaward segment is the area from the open ocean to the shore which must be controlled to support operations and the second area is the landward segment that can be supported and defended directly from the sea (O'Keefe 1992). This approach to Naval operations is stated in the Secretary of the Navy, Chief of Naval Operations, and the Commandant of the Marine Corps policy document that describes the essence of today's Navy as Forward ... From the Sea (Dalton 1994).

These areas of operation introduce new threats and present significantly different problems to the warfare commander. Sensor and weapon systems need to be upgraded to be more effective in such regions particularly in view of the threat of high speed low-level aircraft and missiles such as the air launched Exocet capable of operating less than 50 ft above the sea surface. The sophisticated systems and operational tactics required to combat such threats are impacted by the environment. The use of performance prediction tactical decision aids has become increasingly more useful in support of the warfare commander and his ability to successfully implement his assets. The upper air profile is the critical variable that characterizes the environment and ultimately controls the accuracy of the sensor performance prediction. Thus, it has become increasingly clear that accurately modeling the low altitude

environment is the single most important link to accurately characterizing the performance of a sensor such as a surface-based surface search radar. The system that is currently being utilized at-sea, the balloon launched radiosonde, may unsatisfactorily characterize the low altitude environment providing misleading sensor performance assessments.

The balloon launched radiosonde, that is released from the deck of a Naval vessel, is typically 25 - 30 ft above the sea surface and in the case of an aircraft carrier can be as much as 60 ft above the sea surface. By the time the balloon launched radiosonde is airborne and transmits the first sounding data back to the ship it may be as high as 100 ft above the surface. This vertical gap is extremely dangerous considering the dynamic nature of the environment close to the sea surface. Fluxes in temperature, pressure, and most importantly humidity may vary considerably within this low altitude region yet the balloon launched radiosonde is unable to measure this surface layer. The accurate output from the performance prediction model relies on the quality of the data that is being utilized to model. Using a poor representation of the environment, particularly the lower portion from the surface to 500 ft, will result in either an incorrect or poorly represented sensor performance prediction. The intention of this study is to investigate and compare the quality of refractive assessment obtained with shipboard balloon launched radiosondes and rocketsondes.

The low altitude rocket dropsonde may obtain more fine-scale vertical resolution profiles for use in radar models such as RPO. They also may provide accurate, high resolution refractivity profiles near the ocean surface that deliver better sensor performance model results. The potential for improved assessment near the ocean surface cannot be overlooked particularly in view of the nature of the high speed low altitude threats. It is

paramount that the most accurate resolution of the low altitude profile be utilized in the radar models because ultimately, these products are delivered to the warfare commanders to better assist in their planning and tactical decision making.

B. LOW ALTITUDE ROCKET DROPSONDES

The Low Altitude Rocket Dropsonde System (LARDS) is manufactured by the Atmospheric Instrumentation Research, Inc. (AIR, INC.) located in Boulder, CO. LARDS includes an expendable, rocket-borne meteorological radiosonde and ground-based data acquisition system. The system measures pressure, temperature, humidity, wind speed and direction. The rocketsonde system integrated in the SEAWASP system does not include wind speed or direction. Wind data is not required for propagation loss assessment. This simple low-cost, disposable rocketsonde system was developed using off-the-shelf hobby rocket components. Figure 2.1 shows the rocket in the launcher. The most significant feature of the rocketsonde system is its ability to provide fine-scale vertical profiles. Figure 2.2 shows the higher resolution of a refractivity parameter, to be described later, that is available with the rocketsonde compared to Figure 2.3 obtained from the balloon launched radiosonde that provides temperature, pressure, and relative humidity at intervals of approximately 20 m.

Additionally, the radiosonde obtained near-surface data may be affected by the influence of the ship. It is difficult to obtain accurate environmental data within the immediate area of the ship. A bubble of contamination surrounds the ship created from stack gases, heat generated by the ship, air displacement, and wake caused by the ship's movement (Rowland and Babin 1987). These various items all contribute to contamination that affect the initial sensor reading from the balloon launched radiosonde. Additionally, without proper airflow

through the instrument, the radiosonde may not be properly ventilated and acclimated thus yielding erroneous near-surface data.

The rocketsonde, in addition to providing finer-scale resolution, can provide uncontaminated refractivity measurements down to the ocean surface at some distance away from the ship (see Figure 2.2) which the radiosonde is unable to accomplish. This is illustrated by Figure 2.3 that reveals the large gap in data between the balloon launch point of approximately 60 ft onboard a U.S. Navy aircraft carrier and the surface. This is a significant improvement in data acquisition and particularly enhances the accuracy of radar models at lower altitudes where potential threats from sea skimming cruise and ballistic missiles exist.

In the absence of surface-based ducting from a strong elevated trapping layer, the most important portion of the refractive profile occurs at altitudes below 150 m. Dockery and Goldhirsh (1994) studied two sets of high-resolution atmospheric data collected along the east and west coast of the U.S. and investigated the effects of varying vertical resolution and illustrated the sampling that is necessary to represent significant atmospheric structures. Additionally, they examined the sensitivity of propagation predictions as it related vertical data resolution. These results indicated that a propagation prediction accuracy of 5dB in the low-altitude region would require a vertical resolution of at least 6 m. Vertical resolutions of 18 m and 30 m, which most closely parallel that obtained via balloon launched radiosondes, yield poor representation of the true environment and propagation factor calculations can deviate by as much as 10 - 15 dB.

These results present a need for further study under operational conditions. An

exercise that would provide this type of data is called Ship ASW Readiness and Effectiveness Measuring (SHAREM). A SHAREM is a CNO sponsored exercise program administered by the Surface Warfare Development Group (SWDG). In general, the SHAREM exercise program is designed to measure and evaluate the fleet's ability to conduct Anti-Submarine Warfare (ASW) and the effectiveness of existing ASW sensor and weapon systems. The SHAREM series of exercises were exclusively utilized as a platform for evaluating ASW tactics. The SHAREM 110, that was conducted in the Commander, US Naval Central Command's (COMUSNAVCENT) area of responsibility from 5 to 17 February 1995, was unique in that it incorporated other naval threats and thus the scope of exercise structure was expanded to include multi-threat, multi-warfare scenarios.

One of the primary purposes of participation in this SHAREM exercise conducted in a tactically significant littoral area is to define and understand the environment in which current fleet operations are conducted and potential hostile action may take place. During the exercise a major effort was expended to measure the atmosphere to the maximum extent possible with current techniques and to determine if this level of effort in normal operations was sufficient to characterize the environment. In September 1993, COMUSNAVCENT requested that the Oceanographer of the Navy (CNO/N096) and the Chief of Naval Research (CNR) collaborate in the establishment of an integrated research and development (R&D) effort to develop a methodology and decision aids for the employment of naval Electromagnetic/Electro-optical (EM/EO) sensor and weapon systems to effectively counter critical threats in littoral regions.

Following an October 1993 meeting between CNO/N096 and those organizations

responsible for developing and employing EM/EO systems, the following issues were determined to be the most critical with regards to ship's self-defense and protection of the battle space in the littoral environment: 1) current EM/EO systems must be improved to effectively counter the sea-skimming cruise missiles and low flying aircraft, 2) deficiencies in current EM/EO performance prediction systems should be addressed by capitalizing on commercial-off-the shelf (COTS) technology, 3) efforts shall not result in a major acquisition program nor should it develop new EM/EO systems. The rocketsonde addresses all three of the issues addressed by CNO/N096.

Simultaneous rocketsonde and radiosonde launches during SHAREM 110 provides the opportunity to compare low-level measurements and refractive assessments for a critical littoral area. Data provided from SHAREM 110 will clearly illustrate the huge impact that shipboard influences and measured resolution can have on the performance of surface-based sensors and communication systems.

III. ATMOSPHERIC PROPAGATION

A. INDEX OF REFRACTION

Refraction refers to the property of a medium to bend an electromagnetic wave as it passes from one medium to the next. The degree of bending is determined by the index of refraction, n, which is related to the ratio of the velocity of propagation in free space © to the velocity in the medium (v),

$$n = \frac{c}{v}. \tag{1}$$

Propagation in free space can be related to propagation away from the influence of the earth or other objects. Key concepts concerning refraction will be reviewed following Patterson (1988).

In free space, the rays traced by EM waves travel in straight lines and radars are basically line of sight. This is not true for EM waves traveling in the atmosphere. Even with the assumption of a "normal" atmosphere (i.e. horizontally homogeneous standard atmosphere) radars would still have slightly extended over the horizon detection ranges due to the fact that the index of refraction (n) generally decreases with height. EM waves "bend" toward higher values of n. Rays traveling through the atmosphere are bent toward the surface instead of traveling straight out into space, thus allowing the potential for over the horizon detections.

B. REFRACTION IN THE TROPOSPHERE

The troposphere is considered the primary medium through which radar EM energy propagates. Unlike the ionosphere, the troposphere is not significantly affected by the process of ionization and can be considered an isotropic medium. This means the atmosphere has the same properties in differing directions and the frequency dependency is removed from the index of refraction. The normal value of n for the atmosphere near the earth's surface varies between 1.000250 and 1.000400 (Patterson 1988). For studies of propagation, the index of refraction is not a very convenient number because the value is very close to 1. Therefore, a scaled index of refraction, N, called refractivity, has been defined based on the difference from 1. It is defined as:

$$N = (n-1) * 10^6. \quad \textbf{(2)}$$

The relationship between the index of refraction n and refractivity N for any altitude with atmospheric pressure, P, temperature, T and partial pressure of water vapor, e, is given by:

$$N = \frac{(77.6)}{T} + \frac{(5.6)}{T} + \frac{(3.73*10^5 e)}{T^2}. \quad \textbf{(3)}$$

Both P and e are in millibars (mb), and T is in degrees Kelvin (K). The near-surface or well mixed atmosphere reveals a temperature decrease with height of 10° C per km (dry adiabatic lapse rate). The entire troposphere is characterized by a temperature decrease with height with the average vertical temperature gradient of 6-7° C per km. The only refractive significant gas that varies with height is water vapor. The water vapor content of the

troposphere rapidly decreases with height. Typically at an altitude of 1.5 km the water vapor content is approximately half that of the surface.

Snell's Law predicts the path of an EM ray as it propagates through mediums with varying indices of refraction. It determines the new direction of ray travel as it transitions into a different layer of the medium provided the initial direction of ray travel is known. Snell's law can be used to show that the radius of the ray is determined by the gradient of n using the relationship:

$$r = -\frac{1}{\frac{dn}{dz}}. \qquad (4)$$

Since the propagating EM energy will be bent downward from a straight line as the index of refraction decreases with increasing altitude, a more useful and convenient way of describing the atmosphere's refractive condition is in terms of waves traveling in straight lines. This is accomplished by replacing the actual earth's radius with one approximately four-thirds as great which is typically referred to as the effective earth's radius and by replacing the actual atmosphere by one that is horizontally homogeneous. The resultant refractivity is called modified refractivity (M). The modified refractivity index can be calculated from the following expression:

$$M = N + 10^6 \frac{z}{R_e}. \qquad (5)$$

where z is the height above the earth in km, N is the refractivity at that height and R_e is the

radius of the earth in km. The modified refractivity index typically increases with height in the standard atmosphere. The use of the modified refractivity index is more advantageous to graphically display and identify trapping layers and ducts. Utilization of the refractivity units requires the user to identify where gradients of dN/dz are less than or equal to -157N/km which can often be difficult to identify when N is plotted against height. Also, -157N/km is the vertical gradient that produces ray curvature equal to the earth's curvature. The use of modified refractivity simply requires the identification of negative dM/dz regions to identify the location of trapping or ducting conditions. Figure 3.1 illustrates the typical refractivity, N, and modified refractivity, M, profiles versus altitude for various refractive conditions which will be discussed in the next section and highlights the negative dM/dz gradient required for a trapping layer to exist.

C. PROPAGATION CONDITIONS

1. Standard Refraction

In free space electromagnetic energy will travel in a straight line because the index of refraction is the same in all directions. However, in the earth's atmosphere the velocity of the electromagnetic energy is less than in free space thus the index of refraction decreases with increasing altitude. Therefore, radar generated electromagnetic propagation will be bent downward from a straight line. The refraction occurring in the standard troposphere is referred to as "standard refraction". Since pressure always decreases with height, ray refraction depends primarily on temperature and moisture variations along the propagation path. Standard refraction occurs when dN/dz goes from -79 to 0/km and dM/dz goes from 79 to 157/km. Figure 3.2 illustrates standard refraction as well as the other electromagnetic

wave paths for various refractive conditions discussed in subsequent sections.

2. Subrefraction

If temperature and humidity distributions create an increasing value of N with height, the wave path would actually bend upward and energy would travel away from the earth leading to subrefraction. Subrefraction occurs when temperature and moisture factors combine to cause N to increase with height and dM/dz > 157/km. This situation is less frequent over the water but still must be considered when assessing electromagnetic system performance. The effect on EM sensor systems is reduced detection ranges. Figure 3.2 illustrates the wave path for subrefraction.

3. Superrefraction

If a temperature inversion (temperature increase with height) occurs and/or if the water vapor content decreases rapidly with height, the refractivity gradient will cause the rays to be bent downward more than normal yet less than the earth's curvature. Superrefraction will result in extended radar propagation as illustrated in Figure 3.2.

4. Trapping

If the refractivity gradient is very sharp (less than -157N/km or dM/dz > 0), the radius of curvature for the wave will be smaller than the earth's and the wave will be refracted downward relative to the earth. The downward bending of the EM waves greater than the earth's curvature causes trapping . This trapping or confinement of EM energy acts as a waveguide resulting in extended propagation. Figure 3.2 illustrates this concept of the tropospheric "duct" or "waveguide". Table 1 below summarizes the various refractive conditions for vertical gradients of N and M.

	N - Gradient	M - Gradient
Subrefractive	>0/km	>157/km
Normal/Standard	-79 to 0/km	79 to 157/km
Super-refractive	-157 to -79/km	0 to 79/km
Trapping	<-157/km	<0/km

Table 1. Conditions of Refractivity (after Patterson 1988).

D. ATMOSPHERIC DUCTS

1. General

A duct is a channel in which electromagnetic energy can propagate over great ranges. Propagation of energy within a duct requires that the energy penetrate the duct at angles usually less than one degree. The vertical distribution of refractivity for a given situation as well as the transmitter/receiver location should be considered when assessing a duct's effectiveness.

Ducts provide extended radar detection, UHF communications, and ESM intercept ranges for those systems (i.e. transmitter and receiver) that are operating within the duct. They may also have a significant impact upon systems that cross duct boundaries such as an aircraft operating just above the duct while the radar is located within or just below the duct. Areas of reduced coverage, radar "holes", or shadow zones are all potential problems that could adversely affect radar propagation.

There are numerous meteorological conditions that lead to duct formation. If these conditions occur close to the earth's surface, such that the base of the duct is located at the surface, the duct is a surface-based duct. When the base of the duct is located above the surface it is referred to as an elevated duct. A pervasive ducting mechanism created at the air-

sea interface is known as the evaporation duct which is significant for near-surface propagation paths at frequencies above 2 Ghz.

2. Surface-based ducts

Surface-based ducts occur when the air aloft is exceptionally warm and dry in comparison with the air at the earth's surface. This is most common over the ocean near land masses where warm dry continental air is advected over the cooler water surface. A typical example of this type of advection is the Santa Ana of southern California. These specific meteorological phenomena lead to temperature inversions at or near the surface. In addition, this dry air overlying the moist ocean air can produce a strong moisture gradient which supports the formation of a surface-based duct. Figure 3.3 illustrates the modified refractivity M versus altitude for a surface-based duct created by an elevated trapping layer.

3. Elevated Ducts

Large scale subsidence within oceanic high-pressure systems creates a layer of warm, dry air overlaying a cool, moist layer of air typically referred to as the marine boundary layer. The resultant inversion creates a strong duct at the top of the marine boundary layer referred to as the elevated duct. Figure 3.4 illustrates the modified refractivity M versus altitude for an elevated duct created by an elevated trapping layer.

4. Evaporation Ducts

A change in the moisture distribution with or without an accompanying temperature change can also lead to the formation of a special type of surface-based duct referred to as the evaporative duct. It is the sharp decrease in water vapor pressure from the ocean's surface to a few meters above the surface that creates the large gradient leading to the rapid decrease

in refractive index with height. The evaporative duct height is generally less than 30 m with the world average approximately 13 m (Patterson 1988). Evaporative ducts may also coexist and be found embedded within a thicker surface-based duct.

The proper assessment of the evaporation duct can only be performed by making surface meteorological measurements and inferring duct height from the meteorological processes occurring at the air/sea interface. The evaporation duct cannot be measured using the balloon launched radiosonde, however, employment of the rocketsonde can provide the higher resolution sonde required to measure the evaporative duct more directly. For practical applications however, the turbulent nature of the troposphere at the ocean's surface precludes the characterization of the environment from a single measurement as the refractivity profile measured at one time would most likely not be the same as one measured at another time, even if the measurements were seconds apart.

E. ENVIRONMENTAL DATA REQUIREMENTS AT-SEA

Precise environmental data requirements at sea are difficult to define in terms of the Navy's warfighting capability. This requirement results from environmental data being a part, rather than the end, of the product delivered by the environmental support community. Yet without the basic environmental data the derived environmental products and tactical decision aids tailored for warfare requirements would not be possible. Justification for environmental data should be outlined in terms of improvements to the end or derived product that stem from improvements to data resolution or accuracy. Ultimately it is the improved model accuracy that lends itself to the appropriate application of Naval power and the accomplishment of specific warfare missions.

The importance of tactical shipboard environmental applications can not be overstated. The ability to use and exploit the environment for the specific purpose of carrying out Naval missions is an advantage to the force. The utility of tactical shipboard environmental applications depends on three factors: timeliness, accuracy, and simplicity. The rocketsonde provides improvements in all three of these criteria. Rocketsonde data can be obtained on demand and in less than half the time it takes to prepare and launch a balloon tethered radiosonde. Its vertical resolution of 5 m in all three critical refractive environmental parameters (temperature, pressure, and relative humidity) far exceeds the vertical resolution obtained via the balloon launched radiosonde which can often be as much as 20 m. The radiosonde is capable of providing higher resolution data that would equal that obtained via the rocketsonde however, it is the accompanying data acquisition system that filters and limits the amount of data retained which lowers the vertical resolution and limits the data available for proper assessment of the refractive conditions. Lastly, there is no simpler method to obtain environmental data at-sea than the rocketsonde. The rocketsonde can be launched in any weather conditions regardless of sea state by simply turning the handle of a remotely stationed hand crank. The system can be reloaded for subsequent use in a matter of minutes and there are no other resources required unlike the balloon launched radiosonde that requires helium filled bottles to be embarked onboard ship. Typically a small combatant can only accommodate up to a dozen helium bottles which would require replenishment at-sea during extended deployments. There would be no additional requirements with the rocketsonde other than storage for the rockets and propellant. For shipboard use the rocketsonde provides a much improved tool for rapidly and accurately determining the

refractive conditions.

IV. ASSESSMENT AND MEASUREMENT

A. RADIO PHYSICAL OPTICS (RPO)

The Radio Physical Optics computer software configuration was developed by the Naval Command, Control and Ocean Surveillance Center RDT&E Division located in San Diego, CA. It was prepared for the Space and Naval Warfare Systems Command (PMW-185) Washington, D.C. in September, 1992 in response to Commander-In-Chief, Pacific Fleet Meteorological Requirement (PAC MET) 87-04, "Range Dependent Electromagnetic Propagation Models." RPO version 1.14 was submitted to the Oceanographic and Atmospheric Master Library (OAML) in October 1992. In March 1995, a COMNAVMETOCCOM Independent Model Review Panel (CIMREP) reviewed RPO version 1.14 and recommended changes prior to inclusion in the OAML. The changes recommended by the CIMREP (to be addressed later) were incorporated in RPO version 1.15 which was released in August 1995. In January 1996, RPO version 1.15 was approved for inclusion in the OAML.

The purpose of RPO is to calculate electromagnetic (EM) system propagation loss within a heterogeneous atmospheric medium where the index of refraction is allowed to vary both vertically and horizontally. This marks a significant improvement in propagation loss modeling as the current assessment programs utilized by TESS assume that the troposphere is horizontally homogeneous. RPO propagation loss calculations are independent of any EM system performance considerations (i.e. target size, etc.). RPO calculates and plots propagation loss on a height versus range display for surface transmitters and paths that are

entirely over water. Currently, RPO's ability to only calculate propagation loss for surface-based transmitters marks a significant limitation particularly in view of the military's reliance and use of numerous airborne sensors. It uses a combination of Ray Optics (RO) and Parabolic Equation (PE) techniques to account for range-dependent vertical refractivity profiles.

RPO utilizes a relatively efficient hybrid numerical approach (real-valued sine Fast Fourier Transforms (FFT)) that applies the high-accuracy, computationally intensive parabolic equation (PE) technique in the low-altitude region where refractive effects are the most severe. It relies on geometric optics and extended optics algorithms in the remaining regions. Figure 4.1 shows the four regions and the computational techniques used in each. This approach results in the ability to rapidly calculate propagation loss over large range and altitude regions. RPO is a true hybrid method that uses the complimentary strengths of both the RO and PE methods to construct a fast and highly accurate composite model. In comparing RPO to pure split-step PE models for stressful cases such as those encountered by TESS, RPO was found to be 25 to 100 times faster than the PE model alone with overall accuracy approaching pure PE models.

RPO provides a drastic improvement in propagation prediction accuracy without large execution time requirements. Most importantly, the benefits over the Standard EM Propagation Model, such as that which is currently used in TESS and IREPS, are experienced with or without detailed range-dependent refractivity information. RPO accommodates horizontal and circular polarization over sea water and includes both generic and user-defined height finder antenna patterns. The vertical polarization and surface

roughness algorithms were problems identified by the CIMREP and are yet to be resolved.

RPO's present configuration is capable of accommodating 1 to 33 modified-refractivity versus altitude profiles at arbitrary ranges with up to 51 altitude points per profile. However, the RPO version 1.15 utilized for analysis of the SHAREM 110 data was modified by the Naval Command, Control and Ocean Surveillance Center to handle 1000 altitude points per profile. RPO requires the modified refractivity profile to start at the surface. Acquisition of this surface environmental data (i.e. temperature, pressure, relative humidity) is not obtainable via the balloon launched radiosonde since initial measurements are typically obtained anywhere from 25 to 60 ft above the surface. The balloon launched sounding data then must be extrapolated to the surface from the first two data points in the profile or interpolated using some independent information such as the sea surface temperature. The rocketsonde alleviates this problem by providing the requisite sounding information at the surface. The implementation of efficient and accurate range-dependent propagation models such as RPO demands the high quality environmental data that the rocketsonde is capable of providing and removes the need for data extrapolation or interpolation from balloon launched radiosondes.

RPO operates for frequencies from 100 MHz to 20 Ghz and is applicable for antenna heights from 1 to 100 m. Other significant features include the ability to select: horizontal, vertical, or circular polarization; omni, Gaussian, sin(x)/x, cosecant-squared, generic height finder, or user-defined height finder antenna pattern; vertical beamwidth from 0.5 to 45 degrees; antenna elevation angle from -10 to 10 degrees; tropospheric scatter on or off and gaseous absorption may or may not be included. There are no limits on the maximum altitude

or range for which results can be calculated which is somewhat impractical.

One of the benefits of RPO is that it avoids known deficiencies of the Standard EM propagation model that are currently employed. The Standard Model uses parameterized curves based on series of single-mode waveguide calculations at 9.6 Ghz to describe propagation in the evaporation ducts. These parameterized curves essentially "scale" the 9.6 Ghz waveguide results to other frequencies and duct heights. Similar scaling methods are used to account for surface-based duct propagation. Comparisons with higher-fidelity models, including RPO, show that these scaled results are erroneous in cases involving multi-mode propagation and complicated refractivity conditions. The use of RPO becomes increasingly important as the complicated nature of the refractivity profile becomes evident. This is illustrated by Figure 4.2 using the enhanced vertical resolution available from the rocketsonde. Typical discrepancies resulting from use of the Standard Model include substantial under-prediction of propagation loss values and the crude representation of the "skip-zone" phenomenon in IREPS that is characteristic of moderate-to-large surface-based ducts. Furthermore, the Standard Model does not address effects due to elevated ducts. RPO completely avoids these shortcomings by using a "full-forward-wave" (i.e. the split-step solution to the parabolic wave equation) calculation in the ducting region, which includes all propagating modes and all significant refractivity structures. The most significant shortcoming of the parametric method used in the Standard EM propagation model is that the refractive profiles are used simply to choose the curve corresponding to the pre-calculated refractivity case that best matches the input profile. As a result, important refractive information, such as the specific shape of the evaporation duct profiles and secondary trapping layers are

completely neglected. RPO has no intrinsic limit on the complexity of the refractivity profile, and properly represents the propagation effects resulting from all structures in the profile within the PE region. As mentioned previously one of the most important features of RPO is that it will accommodate range-dependent refractivity conditions via specification of several profiles at different ranges. Although measured profiles at differing ranges are rarely available at present, the importance of range-dependent effects is acknowledged, particularly in littoral regions, and there are several potential future sources of range-dependent data such as numerical weather prediction models, multiple measurement platforms, lidar, and remote sensing. Lastly, since RPO is based principally on physical models, future upgrades involving the inclusion of more accurate algorithms are much more likely to be feasible. This is not the case for a model such as the Standard EM propagation model which is a non-physical parameterization of results from other models.

There were two significant improvements to RPO version 1.14 that are incorporated in RPO version 1.15 that subsequently led to its acceptance into the OAML library. The first is that it was modified to include the first-order effects of gaseous absorption. In the Extended Optics (XO) region, rays are only allowed to travel upward. Thus, it is impossible to either trap energy within the XO region or recombine energy from the XO region with energy in the PE region. The second item addressed in version 1.15 is the ability to identify and display the height of the PE/XO boundary (PE max, Figure 4.1) on the RPO output screen. This was significant particularly because it was noted that ducting in the XO region will not be modeled. This now allows the operator to compare the height of the bottom of the XO region with the highest trapping layer at any range. If a trapping layer is noted to be above the base

of the XO region, the operator will be properly warned of the potential for errors.

Future developments of RPO that would ultimately allow replacement of the range independent propagation loss model in TESS as well as other tactical decision aids are progressing rapidly. The first improvement on the CIMREP list is the use of proper boundary conditions for vertical polarization and the incorporation of a surface roughness algorithm. The Terrain PE Model (TPEM) will be combined with RPO version 1.15 and will be released as IREPS 4.0. This will allow for calculation of propagation loss for transmitters and targets at any altitude. For cases involving elevated ducting, specific work is being focused on the development of a model to more accurately handle the airborne transmitter and target scenario located within the duct.

1. Vertical resolution

The successful development of accurate range-dependent models has led to the challenge of obtaining high resolution data for effective system performance predictions. In particular this focus will look to address the minimum acceptable resolution in the vertical direction. A case study is necessary to examine whether the vertical resolution, 5m, provided by the rocketsonde meets or exceeds that which is required for accurate characterization of the refractive environment. An examination is also necessary to show that the lower vertical resolution provided by the Marwin Rawinsonde Set (MRS) utilizing balloon launched radiosondes does not favorably represent the actual environment and ultimately could lead to misleading structures in the environment that would severely impact propagation assessment.

The sensitivity of propagation factor predictions to measurement resolution was

examined by manipulating the raw atmospheric data to reduce vertical resolution and subsequently repeating the calculations. The case study (Dockery and Goldhirsh 1994) involves data collected by a civilian helicopter equipped with atmospheric sensors which collect temperature, pressure, and humidity versus altitude data. The data was collected during a U.S. Navy exercise conducted near San Nicolas Island off the coast of Southern California on 19 March 1988. The helicopter recorded data at a 2-Hz rate on each descent and had a descent rate of 100 to 150 m per minute resulting in data being recorded at intervals less than 1 meter in altitude.

Data collected in this manner provide excellent agreement with observed signal levels and system performance and thus the helicopter-acquired atmospheric data is assumed to be the baseline or "ground truth". It is assumed that the helicopter measurements have sampled the atmosphere on a fine enough grid to support near perfect reconstruction of the propagating signal. An algorithm called LARRI (Large-scale Atmospheric Refractivity Range Interpolator) was used to smooth the individual refractivity profiles, extrapolate to the surface, find the best possible match of refractivity structures between adjacent profiles, and interpolate between profiles while preserving matched structures. The propagation model used during the investigation was TEMPER (Tropospheric Electromagnetic Parabolic Equation Routine) which is based on the Fourier split-step numerical solution of the parabolic wave equation. Parabolic models such as RPO and TEMPER, as used in this analysis, are the only models that have demonstrated robust performance in complicated range-varying refractive environments. The study focuses on altitudes below 150 m where refractive effects on propagation are most severe. The San Nicolas profiles exhibited low and moderate altitude

ducts (35-110 m) with a significant amount of structure and considerable lateral inhomogeneity. Figure 4.3 illustrates the eight refractivity profiles collected with the instrumented helicopter over a 65 km range. Figure 4.4 shows the smoothed and interpolated profiles generated by LARRI for use in TEMPER for the San Nicolas Island case.

The sensitivity of propagation factor predictions to measurement resolution is examined by manipulating the raw atmospheric data to reduce vertical resolution and subsequently repeat the TEMPER calculations. The results of the "manipulated" vertical resolution are compared with the "ground truth" calculations to determine impact. The first refractivity profile from Figure 4.3 was chosen as the single profile for the vertical resolution calculations. The profile exhibits two distinct ducting layers at 35 m and 110 m. The average vertical spacing between helicopter data over the first 150 m of the sounding was .6 m. Lower resolution measurements were simulated by retaining only every ith (e.g. I=10,30,50) measurements from the original sounding and repeating the TEMPER calculations with the modified sounding. Keeping every 10th, 30th, and 50th point results in vertical resolutions of 6 m, 18 m, and 30 m, respectively. The original and thinned profiles after smoothing are plotted in figure 4.5. The systematic degradation of the original data is evident with only the 6 m case being a relatively faithful reproduction of the .6 m profile. The profile with 30 m resolution shows a weak, 100 m surface duct that exhibits none of the structure of the original data. The comparison of the 6 m and the 18 m/30m results will be similar to that obtained via rocketsonde and radiosonde, respectively. The Goldhirsh and Dockery comparison of the 6 m and the 18 m/30 m results will be used in this study to interpret rocketsonde versus radiosonde derived results.

TEMPER propagation factor calculations were performed for each of the profiles in Figure 4.5 using a 20 m antenna height and frequencies of 10 Ghz and 3Ghz. In order to investigate the effects of degrading measurement quality, the vertical profiles were examined at ranges of 30 km and 50 km respectively. The results for the 10 Ghz frequency are shown in Figure 4.6. At the 30 km range the propagation factor for the original or "ground truth" profile exhibits a fade region of 15 dB or more between 45 m and 80 m. This is the altitude region between the two ducting layers in the refractivity profile. The 30 m resolution results show very little structure through this region, which is consistent with the over-simplified refractivity profile in Figure 4.5. The two intermediate resolutions are deviating from the baseline by 5 to 10 dB between 50 and 95 m at 30 km. Overall, the 6 m resolution results are noticeably better than the 18 m results below 40 m.

Viewing a slice of the refractivity profiles at 100 m over a 50 km range allows for analysis of range-dependency in conjunction with variations in the vertical resolution. Figure 4.7 shows the propagation factor calculations by TEMPER for a 10 Ghz antenna at 100 m altitude. The results indicate the 6 m vertical resolution more closely parallels the .6 m baseline measured propagation factor. The results at 30 m are extremely poor exhibiting errors as high as 15 dB at a range of 35 km. The 18 m results are off baseline by 10 dB whereas the 6 m results are only off by 5 dB.

This study highlighted the sensitivity of propagation predictions to measurement resolution. In particular it highlights the importance of good refractivity data in the vicinity of laterally inhomogeneous, low altitude surface ducts and the huge impact it can have on the performance of surface-based sensors and communication systems. Based on the 10 GHz

propagation in the March 19, 1988 San Nicolas conditions, one would conclude that to maintain a propagation accuracy of 5 dB in the low-altitude region requires a vertical resolution of at least 6 m.

B. ROCKETSONDES

The low altitude rocket dropsonde system or rocketsonde is a refractive measurement device developed using off-the-shelf hobby rocket components. Figure 4.8 shows the rocketsonde assembly in the launcher and the data acquisition computer system during a launch from a U.S. Navy aircraft carrier. The interest in the development of the rocketsonde was initiated by the Atmospheric Technology Branch of the U.S. Army Test and Evaluation Command's (TECOM) Atmospheric Sciences Division (ASD) located at the U.S. Army White Sands Missile Range, NM to satisfy the requirement for high accuracy and high resolution low altitude meteorological data from unmanned, remote locations without the use of helium balloons. The rocketsonde is readily available, reliable off-the-shelf technology that has been successfully tested and operationally used at-sea onboard U.S. Navy vessels to telemeter fine-scale measurements of temperature, pressure, and relative humidity.

Figure 4.9 shows the component parts of the rocketsonde including the rocket body, nose cone, engine, and instrument package attached to a parachute. The micro-processor controlled digital sensor package is carried aloft in a 63.5 mm diameter non-metallic rocket that is fabricated of paper and plastic. The rocket motor also contains no metal and utilizes a solid propellant that is safe to store and transport. The total weight of the rocket vehicle and payload is less than one pound. The body of the rocketsonde is fabricated of inexpensive composite material and plastic. It contains no hard metal parts that could be hazardous to

personnel or property. The rocket motor case is a fiber wound, phenolic impregnated tube. Under Federal Aviation Administration regulation FAA 101, no special approval is required to launch rocketsondes as they are classified under the same rules as hobbyist model rockets. None the less, they should still be considered high velocity projectiles as they are capable of accelerating to 0.5 mach speed in 2-3 seconds. Table 2 below details the rocketsonde characteristics.

Rocket length	66 cm
Rocket diameter	63.5 mm
Total launch weight	453 g
Instrument package weight	113 g
Parachute size	91.4 cm
Rocket propellant	Ammonium percholate-polyurethane
Propellant weight	56 g for 757-m altitude
Total cost per shot:	$ 200

Table 2. Rocketsonde Characteristics

Due to the descent rate of 2 m/s after parachute deployment, fast response sensors are necessary. The accuracy, response time, and resolution of the pressure, temperature, and relative humidity sensors approaches that of high quality laboratory instruments. Pressure and humidity sensors each respond in one second or less while the temperature sensor responds in approximately 3 s. Pressure as measured by the rocketsonde is accomplished via a dual diaphragm aneroid capacitance transducer. The pressure sensor's small temperature dependance is compensated for by a temperature-sensitive capacitor mounted near the sensor.

The pressure sensor is insensitive to shock, vibration, acceleration, and orientation. It senses pressure accurately even under the shock and acceleration of 20 to 50 g's at launch.

A small Negative Temperature Coefficient (NTC) bead thermistor is used for temperature measurement providing high sensitivity, fast response, and long-term stability. The sensor is coated with a water-proof, reflective material which reduces the effects of solar radiation.

Relative humidity is measured by a thin polymer membrane capacitance sensor. This sensor is extremely stable and linear. Even extended exposure to 100% relative humidity has little effect on stability. The sensing polymer is 2 microns thick and exposed to airflow on both surfaces; the time constant response to relative humidity fluctuations is less than one second. Specifications for the sensor performance are listed below in Table 3.

PRESSURE SENSOR	
Type:	Aneroid capacitance
Pressure Range:	1050 to 600hPa
Accuracy:	1.0hPa
Resolution:	0.01hPa
Response Time:	<0.1 second
TEMPERATURE SENSOR	
Type:	Bead thermistor
Temperature Range:	-55° C to 50° C
Accuracy:	0.3° C
Resolution:	0.01° C
Response Time:	>1.0 seconds

HUMIDITY SENSOR	
Type:	Capacitance polymer
Humidity Range:	0 to 100%
Accuracy:	3% RH
Resolution:	0.1% RH
Response time:	<1.0 seconds

Table 3. Rocketsonde Sensor Performance Characteristics

A microprocessor within the rocketsonde measures pressure, temperature, and relative humidity (PTH) each second using RC oscillators and frequency counting circuitry. PTH sensor calibration coefficients are stored in the sonde's memory and transmitted along with measured sensor data. The rocketsonde transmits a 100 milliwatt crystal-controlled narrow band 400-406 MHZ frequency that provides a range of 160 km. The sonde is housed in a thermally insulated, light weight, small volume, styrofoam package and is powered by two standard 9 volt batteries which provide sufficient energy for a two to three hour flight.

The ground station consists of three elements: UHF receiver, GPS wind processor (latest version), and an IBM compatible PC. The PC is an unmodified commercial, personal computer. The application software was written to run under the IBM OS-2 operating system which allows for multi-tasking and seamless manipulation of both tabular and graphical real-time data. A single RS-232 COM port provides the interface between the PC and the system. The processor within the receiver has two microcomputers that receive and process telemetry data continuously. One converts the encoded telemetry signal into standard binary data. The second calculates pressure, temperature, relative humidity, and time in standard scientific units. The UHF FM receiver was specifically designed for rocketsonde telemetry reception. Receiver functions are controlled through the RS-232 port or the front panel keyboard. This

allows the ground station computer to scan the meteorological frequency band and warn the operator of potentially interfering signals within the band. With standard coaxial cable, the omnidirectional antenna and preamplifier can be separated from the receiver up to 100 ft.

After the rocketsonde is electrically ignited by a quick crank on a hand generator and launched, it travels at approximately 0.5 mach and reaches its peak altitude of one kilometer (latest GPS version peak altitude is 10,000 ft) in less than 10 seconds. Upon reaching peak altitude, the ejection charge deploys the instrument package which slowly descends beneath its 1-meter parachute at a nominal rate of 2 m/s while the nose cone and rocket body tumble safely to the surface. Every 1-2 seconds the rocketsonde sensor package telemeters pressure, temperature, humidity, and reference data using the FM narrowband crystal-controlled transmitter. The slow descent and high sampling rate of the sonde, provides a high spatial and temporal resolution profile of the atmosphere. The rocketsonde system software that is loaded on the IBM OS-2 portable PC handles the data acquisition and processing. Computations are performed to convert the rocketsonde sensor data into meteorological values. The parameters of pressure, temperature, and relative humidity are utilized to calculate the refractive index which is subsequently converted to a modified refractivity which can be graphically displayed and used to identify various refractive conditions.

C. MRS RADIOSONDES

The current method of obtaining environmental parameters onboard U.S. Navy ships at-sea is with the MARWIN MW 12 Rawinsonde Set (MRS) manufactured by Vaisala. The MARWIN MW 12 is a portable rawinsonde set designed to support different facets of

defense operations. The set is small, lightweight, easily portable and rapid to deploy. It is rugged and well protected for use at-sea. The design ensures accurate passive measurement of upper-air wind direction and speed, pressure, temperature, and relative humidity up to altitudes of 30 km. Vaisala is the most widely used and largest manufacturer of complete upper-air systems with over 90 countries utilizing their systems worldwide. The MRS, as illustrated by Figure 4.11, processes data obtained from the RS 80 Series radiosondes. It is a sounding instrument mounted in a metal-reinforced polyurethane enclosure with closed circuit cooling and shock absorbers. It comprises of a power supply, radiosonde receiver, signal filters, PTU and wind data processors, CPU, and a program storage unit. The MRS is a portable unit that meets the specific needs of obtaining environmental data, particularly the quantities of pressure, temperature, and humidity required for refractive assessment, onboard ships at-sea.

The MRS system is installed in a lightweight aluminum case painted green. The front cover is detachable and the enclosure is provided with shock buffers to separate the inner case from the outer shell. This protects the electronics during transportation and use in high-vibration environments. Although the system is built to withstand the rigors of frequent transportation and use at-sea, it should be noted that several problems were encountered during use with Mobile Environmental Teams (MET). The MET operate onboard ship's at-sea for periods of time ranging from 2-3 days up to 6 months. The frequent requirement to embark and debark ship's has placed added stress on the system and problems have ensued ranging from electronic circuit component failure to sonde calibration coefficient discrepancies. These types of problems are encountered much less frequently onboard ships

such as aircraft carriers that have the system permanently mounted. For this study the focus will be on the radiosonde, its components, and launch procedures and equipment.

The Vaisala RS 80 series of radiosondes was designed to be small, lightweight, fully solid state, and easy to handle. The radiosondes have sensors to measure pressure, temperature, and humidity. The RS 80 sondes operate in the 403 MHZ frequency band. The RS 80-15N is the sonde utilized by the U.S. Navy and is able to provide PTU parameters as well as Omega Navaid windfinding. The RS 80-15N is illustrated in Figure 4.12. The specific features of the RS 80-15N radiosonde are provided below in Table 4.

Size	55 x 147 x 90 mm
Weight	Less than 200 g
Sampling Rate	1.5 sec (all parameters)
Solid State Construction Design	High technology BAROCAP, THERMOCAP and HUMICAP sensors
Total cost per launch	$150 (includes balloon,helium,radiosonde)

Table 4. RS 80-15N Radiosonde Characteristics

The RS 80 radiosondes have been used for routine upper air observations since early 1981. The mechanical construction provides a small, lightweight, and solid state sensor that is insensitive to mechanical stress, dirt, and humidity. Each sonde is packed in a hermetic metal foil bag that also contains a magnesium-cuprous chloride water activated battery . For good exposure to free air the temperature and humidity sensors are mounted close to the tip of a support made of flexible circuit material. The support is insulated and coated with thin electrically grounded aluminum film and finally treated to be water repellant. The humidity

sensor is additionally provided with a cap to protect it against direct impact of water droplets and solar radiation. The unique Barocap pressure sensor is mounted as a component on the transducer electronics board. This new type of transducer is fully self-contained and needs no external installation frame. It provides a continuous and unambiguous pressure reading over the full range of operation. The completely welded structure is very rugged and tolerates transportation shocks better than any previous radiosonde pressure sensor. Temperature dependence is very low, approximately 4 mb over 100° C range.

The set of solid state sensors consists of an aneroid capsule (BAROCAP) with capacitive transducers in the inside vacuum, a ceramic temperature sensor (THERMOCAP) and a thin film humidity sensor (HUMICAP). All of the sensors are capacitive with compatible dynamic ranges which essentially simplifies the transducer electronics. In the radiosonde only one reference capacitor is needed to eliminate the influence of drift of transducer electronics.

The pressure sensor is a small aneroid capsule with capacitive transducer plates inside. The external diameter of the capsule is 35.5 mm and the weight of the complete assembly is 5 g. Figure 4.13 illustrates the BAROCAP pressure sensor. Transducer plates are supported by membranes made of special steel alloy. The supporting rods of the plates are fixed to the membranes with hermetic glass-to-metal seals. The inverted construction is used to obtain maximum sensitivity at low pressure. The transducer electronics senses the capacitance between the plates only, with no influence of stray capacitances between the plates and the membranes, which are grounded. Some advantages of the construction are there are no joints in the construction which could slip when the sensor is exposed to mechanical stresses.

Neither does the construction contain any springs, arms, contacts or assembly frame that was common in old designs. The transducer plates are protected against moisture and dust. Additionally, the absence of an assembly frame and small sensor size has made it possible to achieve a very small temperature dependence, that is, with changing temperature the temperature differences stabilize fast.

The temperature sensor (THERMOCAP) is based on dielectric ceramic materials, the temperature dependence of which can be accurately controlled with selection of materials and processing parameters. Figure 4.14 illustrates the THERMOCAP temperature sensor. Metal electrodes are formed on both sides of a tiny ceramic chip. The capacitance between the electrodes is a function of temperature. To ensure complete moisture protection the sensor is hermetically sealed in a small glass capsule with two connecting leads. To avoid uncontrolled stray capacitances which could be caused by water droplets on the glass capsule, an electrically grounded thin film aluminum coating is deposited on the sensor capsule and leads. This coating also has excellent radiation properties for minimizing the radiation error of the observation. An insulation layer on the leads prevents short circuits.

The HUMICAP humidity sensor is a thin film capacitor with a polymer dielectric. The polymer is about 1 micron thick. The sensor capacitance is dependent on the water absorption in the sensor's dielectrical material. Figure 4.15 illustrates the HUMICAP humidity sensor. The sensor is fabricated using thin film technology similar to that used in microelectronics. The sensor is small (4x4x0.2 mm), hence its thermal mass is also small and the sensor very closely and quickly follows the ambient air temperature. This is obviously necessary for obtaining true relative humidity values in the atmosphere. Other attractive features of the

sensor are fast response, good linearity, low hysteresis and small temperature coefficient. The sensor operates reliably in low temperature to at least -60° C. Specifications for the radiosonde's sensor performance are listed below in Table 5.

PRESSURE SENSOR	
Type:	Capacitive aneroid
Pressure Range:	1060 to 3 hPa
Accuracy:	0.5 hPa
Resolution:	0.1 hPa
TEMPERATURE SENSOR	
Type:	Capacitive bead
Temperature Range:	-90° C to 60° C
Accuracy:	0.2° C
Resolution:	0.1° C
Lag:	< 2.5 seconds
HUMIDITY SENSOR	
Type:	Thin film capacitor
Humidity Range:	0 to 100%
Accuracy:	2% RH
Resolution:	1.0% RH
Lag:	1.0 second

Table 5. RS 80-15N Radiosonde Sensor Performance Characteristics

The RS 80 radiosonde includes an unwinder with 30 m of string. The unwinder also referred to as the spool-off device is attached directly to the neck of the balloon. The unwinder string length improves the accuracy of temperature measurement as it ensures that the radiosonde is always outside the balloon thermal wake regardless of launch conditions. Part of the difficulty with utilizing balloon launched radiosondes particularly in high wind conditions is the length of the unwinder assembly. The 30 m of string, that must unravel from the assembly before the radiosonde becomes airborne, often causes the radiosonde to bounce

or impact the ship's deck or other superstructure such as a gun mount. This type of impact can severely degrade the calibration of the sensing components as well as frequently cause a total loss of transmission of environmental data. Even a low wind situation can create difficulties with launching balloons from ship's at-sea. The turbulence created in the boundary layer particularly in the vicinity of the ship's wake can often cause the balloon and attached radiosonde to impact the ship or even be driven into the water.

Another limitation of using the balloon launched radiosonde is the requirement to co-locate the MRS in close proximity to the helium bottles which on small combatants is usually located in the helicopter hangar. This can make balloon launching very difficult particularly if the technician has to fill the balloon in the hangar, walk the helium filled balloon out to the edge of a flight deck with gusty winds and attempt to get the balloon successfully off the flight deck without collision or impacting the water.

Although dry-bulb temperatures can be made aboard ship with relative ease, it is difficult at best to achieve good accuracy. Roll (1965) examined many of the difficulties of making precise measurements of meteorological variables at-sea aboard large research vessels and found that an important problem is the effect of ship heating upon temperature measurements. The heating results from the absorption of solar radiation by the ship (Goerss and Duchon 1980). Goerss and Duchon investigated the ship heating effect and subsequent error in ship surface measurement systems during GATE. The ship heating effect, particularly in the afternoon, was found to induce as much as a 2° C error in the measured dry-bulb temperature data (Goerss and Duchon 1980). The ship heating effect must be taken into account in order to derive meaningful estimates of the error content of shipboard

measurement systems.

Lastly, a case study looked at the inaccuracies in radiosonde data arising from the relative accuracy between the surface point data and the radiosonde (Helvey 1983). Standard observation procedures in the U.S. Federal Meteorological Handbook for Radiosonde Observations (FMH-3) specify use of psychrometer data for the surface point data. Onboard U.S. Navy vessels these measurements are typically taken from the bridgewing by the Quartermaster of the Watch. This means that the relative accuracy between sonde and psychrometer becomes a determining factor in the accuracy of the refractive gradient for the lowest layer of the profile. Combining this factor along with the potential errors that may be induced due to exposure to various environments (i.e. cooler or warmer environments) and poor acclimation prior to launch can result in poor representation of the refractive gradient for the lowest layer of the profile. For example, consider Figure 4.16a that shows an idealised daytime atmospheric temperature profile labeled "T". The broken-line curve marked "C" represents the thermal response of the hygristor and initial negative offset caused by recent exposure to a cooler environment. The curve marked "W" represents temperature of a hygristor with an initial positive offset as might be caused by solar heating prior to release. Figure 4.16b shows the corresponding curves for humidity or refractivity error with height. In either case errors owing to thermal lag and sensor adjustment would tend to yield similar relative departures from true conditions depending on the sign of the lag effect. This ultimately would lead to gross errors in the calculated refractive conditions and ultimately poor assessment of a sensor's performance. The latest sonde version utilized by the MRS does not use a hygristor. However, this example illustrates the importance of sonde

component acclimation prior to launch.

Part of the problem with radiosonde usage onboard ship is that it does not receive satisfactory airflow of uncontaminated air through the sensor elements while it is at rest on the deck or in the hands of a technician just prior to launch. The rocketsonde approach ensures that satisfactory airflow and sensor adjustment to atmospheric conditions is accomplished prior to measuring the atmospheric parameters at the lowest levels thus ensuring proper assessment of the refractive conditions. Additionally, since the measurements are taken continuously through descent until it reaches the surface, there is no concern for mismatched gradients between two different sensors such as what is obtained when utilizing balloon launched radiosondes.

D. COMPARISON OF RADIOSONDE AND ROCKETSONDE MEASUREMENTS

There are tremendous advantages in using the rocketsonde for refractive assessment. As discussed previously, an air mass may be nearly horizontally homogeneous in refractivity but, refractivity is not homogeneous in the vertical. Vertical distribution of atmospheric data plays an important role in the accurate characterization of the environment. The balloon launched radiosonde currently used onboard U.S. Navy ships ascends at approximately 4 m/s and provides the atmospheric parameters of temperature, pressure, and relative humidity roughly every 16 to 18 m. The rocketsonde on the other hand has a much slower descent rate (2 m/s) and is able to provide data at intervals of 5 m or less. Figure 4.10 illustrates the significant difference in vertical resolution and possibly the impact of ship contamination for M unit profiles obtained from a simultaneously launched radiosonde and rocketsonde. The

significance of this improved vertical resolution as well as the other advantages in conjunction with the rocketsonde will be highlighted by RPO outputs provided in a later section.

One of the biggest problems that the radiosonde presents is its exposure at the surface and the subsequent errors it can provide by not having the sensors properly acclimated. Even when reasonable care is exercised to avoid prolonged exposure to direct sunlight, appreciable warming of the instrument case and hygristor is probable, because of poor ventilation while the sonde is held stationary during the period just prior to release. This temperature excess will persist for some distance above the surface, prolonging and increasing the magnitude of the error in calculated refractive index. It is not until the sensor is fully acclimated with proper ventilation that one can expect reasonably accurate measurements from the radiosonde. Thus the data obtained at the lower levels particularly just after launch is typically not a good representation of the actual environment. This same principle applies to the rocketsonde in that the data initially obtained after the rocket has reached peak altitude is not reasonably accurate because the sonde's sensors have not become completely acclimated. This is not as big of a problem as with the radiosonde for it is the data in the lower levels near the surface that is most important and by the time the rocket has descended to these levels the sensors are fully acclimated and are providing accurate measurements. Similar consequences will follow introduction of a radiosonde into a relatively cool outdoor environment after preparation inside a warm enclosure. Radiosondes are often released before becoming fully acclimated to the prevailing warm, moist natural conditions outside. Other sources of radiosonde error will be discussed in the next section.

Another advantage for using the rocketsonde is that it does not require the use of helium. Shipboard atmospheric profiling utilizing balloon launched radiosondes requires the use of helium. Most U.S. Navy ships are not equipped with helium resources thus the helium bottles must be transported to the ship and appropriate storage space which is often very limited onboard ship must be identified; also arrangements have to be made for replenishment at-sea as required during longer deployments. The rocketsonde eliminates the need for helium and the storage space required for the rockets and rocket motors would be minimal and no inconvenience to limited shipboard storage facilities.

Balloon guided radiosondes launched from ships at sea provide contaminated measurements in the vicinity of the ship due to discharge of ship's effluence and large heat signature as well as changes in the environment immediately surrounding the ship. A bubble of contamination surrounds the ship created from stack gases, heat generated by the ship, air displacement, and wake caused by the ship's movement.

Augstein et al. (1974a), in a comparison of data taken simultaneously from the deck of a ship and from a buoy, concluded that the ship's hull and superstructure induced sizable distortions in simple measurements of air temperature, humidity, and wind speed. Hoeber (1977), in a specially designed experiment in which data were taken simultaneously from the deck and from the forward boom, found that even rudimentary shipboard measurements (including barometric pressure) were very difficult; he estimated that the errors in some of the resultant bulk-derived fluxes were on the order of 100%. Goerss and Duchon (1980), with an arrangement similar to that of Hoeber, observed air-temperature difference errors, during the GATE experiments, of more than 2 degrees C, due to a heating influence of the ship

during the day. Reed (1978) reported similar results. The rocketsonde, on the other hand, obtains uncontaminated measurements at some distance away from the ship's influence thus eliminating potential errors in measured pressure, temperature, and humidity. This advantage alone establishes the rocketsonde's data as far superior to that which is obtained via ship launched radiosondes.

The rocketsonde can be considered an all-weather instrument capable of providing meteorological data regardless of sea-state or wind conditions. If the winds and seas are too high, it may preclude a technician from working topside on a small combatant and would not allow for the launching of weather balloons. If winds are too high, it often becomes too difficult to get a balloon inflated and launched without bursting. On the other hand, the rocketsonde can be remotely launched without jeopardizing the safety of a technician working topside during adverse weather conditions. In contrast, the rocketsonde will easily launch and operate regardless of wind or sea conditions. This presents a significant tactical problem in that often times during exercises in adverse weather conditions, afloat commanders are without radar propagation assessment information due to the inability to launch balloon guided radiosondes. Lastly, the launching of weather balloons often requires adjustment of the ship's course to preclude the balloon from getting trapped in the ship's superstructure. In addition, maneuvering the ship, particularly small combatants, is frequently required to reduce the relative winds across the flight deck in order to get the balloon released without bursting or taking off errantly and bouncing off the ships deck or superstructure. The use of the rocketsonde would eliminate any need for the ship to maneuver.

A typical balloon launched radiosonde requires 20 to 30 minutes for preparation,

balloon filling, and release and it may take another 30 to 45 minutes to obtain the requisite data for analysis. The rocketsonde can be pre-staged and ready for launch and the start-up sequence requires only a few seconds. This eliminates any specific preparation and the data can be obtained within 15 minutes after launch. It is also ideal for taking multiple soundings in rapid succession as the launcher can be reloaded immediately. This provides the ability to increase the spatial sampling and lateral data resolution which supports the range-dependent propagation models. Lastly, since the rocketsonde can be pre-staged and ready for launch atmospheric sounding data for environmental characterization can be obtained on command. For example, if the battle group commander desires refractivity conditions based on current sounding data, a rocketsonde can be immediately launched and processed environmental data and refractive conditions can be obtained within 15 minutes.

Probably the most significant contribution the rocketsonde provides is its ability to measure environmental parameters at the surface which yields the zero height information of pressure, temperature, and relative humidity required for the RPO model. If shipboard prediction systems such as TESS are going to incorporate range-dependent vertical refractivity profiles, a data acquisition system such as the rocketsonde capable of measuring the zero height profile must be incorporated.

There are two disadvantages of the rocketsonde that have been noted. First, the rocketsonde is still an expendable commodity. The use of expendables becomes costly and requires continuous replenishment particularly during extended periods at-sea. It should be noted, however, that both the rocketsonde and radiosonde are comparable in price. The rocketsonde is slightly more expensive than the radiosonde ($200 vice $130) but price

difference is primarily due to limited rocketsonde production. With mass production, the rocketsonde price would more than likely decrease to equal the price of the radiosonde. Ultimately, the use of permanently mounted shipboard sensors that would provide continuous atmospheric profiling with improved vertical resolution is required to meet the environmental data requirements at-sea.

Secondly, the rocketsonde in its current version does incorporate the Global Positioning System (GPS) wind finding technique but is only capable of reaching altitudes of approximately 10,000 ft. For the rocketsonde to be a suitable replacement for the balloon-launched radiosonde, it would have to reach altitudes in the vicinity of 20 to 30,000 ft as this upper-level information is vital for aviation parameters and flight forecasting. The rocketsonde is currently being developed to reach such altitudes. It is expected to be ready for operational testing within a year.

V. ENVIRONMENTAL DATA FOR STUDY

A. SHAREM 110

Data for study were obtained in a special SHAREM, SHAREM 110. SHAREM 110 Phase 1 was designed to be a complex, multi-warfare exercise conducted in the COMUSNAVCENT Area of Responsibility (AOR). This SHAREM was one of a continuing series of exercises initiated in January 1993 to combat the submarine threat in the region. Recently, the exercises have been expanded and revised to address all warfare areas.

The primary purpose of the EM/EO participation in SHAREM 110 Phase 1 was to demonstrate in a tactically significant theater of operations an end-to-end Meteorological and Oceanographic (METOC) support system. The EM/EO support system consisted of two components, the SPAWARSYSCOM METOC Shipboard Forecast Tactical Atmospheric Capability (STAFC) and Sensor Performance Prediction Advanced Development Model (SPP-ADM).

The STAFC combined normal Fleet Numerical METOC synoptic forecast production runs with new, higher resolution mesoscale forecast fields to provide regional forecasts to an upgraded TESS workstation located in Bahrain. The TESS workstation utilized the Fleet Numerical METOC Center forecasts, updated by local shipboard observations, to provide EM propagation information required aboard the EM/EO test ship to run RPO EM propagation loss model. This propagation loss information was provided to the SPP-ADM system aboard the EM/EO test ship (USS Lake Erie) and used to generate sensor performance/assessment products. During the SHAREM exercise, SPP-ADM used the output of the RPO

propagation loss model as the primary basis for performance predictions and assessments. The RPO model used as input a combination of historical databases, synoptic and mesoscale forecast information and in-situ measurements as part of the EM/EO support system to provide the most accurate performance prediction and assessment possible.

The support system process, utilized during the exercise, was initiated by high resolution FNMOC models transmitted to Bahrain where they were interfaced with in-situ measured environmental inputs and transmitted to the USS Lake Erie. This data was combined on the ship with the most recent measurements and measured clutter data to finally result in shipboard generated radar performance predictions. The EM/EO support system made use of state-of-the-art prediction models such as the Naval Operational Regional Atmospheric Prediction System (NORAPS), extensive and exhaustive measurements using sophisticated measurement devices and exchange of substantial amounts of data (both modeled and measured) to provide near real time predictions of Combat System performance. Figure 5.1 depicts the overall data flow and communications connectivity for the EM/EO support system during SHAREM 110.

The difficulties in obtaining valid atmospheric measurements on ships during this as well as past exercises has been identified as a major source of error for accurate prediction of EM/EO system detections (Integrated Performance Decisions 1994). The effect of each ship's air envelope because of wind flows over the ship structures and thermal heating of the ship's mass, and location of the instrumentation with respect to solar radiation are all contributing factors.

The surface ships which participated in SHAREM 110 were the USS Lake Erie

(LKE), USS David R. Ray (DRR), USS Vandegrift (VAN) and the USNS Silas Bent (BNT). The Officer in Tactical Command (OTC) was Commander, Destroyer Squadron Fifty (COMDESRON 50) embarked on the USS David R. Ray. There were two operating areas during SHAREM 110. The first half of the exercise was conducted in the southern Persian Gulf and the second half was conducted just outside the Strait of Hormuz in the western Gulf of Oman.

An extensive atmospheric data collection effort was executed as part of the OP-096 sponsored EM/EO Support System demonstration. This included 130 minirawinsonde launches from three different platforms (LKE, DRR, BNT), 15 dropsonde launches from the USS Lake Erie's LAMPS MK III helicopter, 28 rocketsonde launches, and 9 floatsonde launches from the USS Lake Erie in support of the SEAWASP (SPY-1B performance prediction system) system demonstration, and a total of 3000 valid surface observation measurements (sea surface temperature, dew point depression, and wind speed/direction) using the Surface Ship Atmospheric Weather Station (SSAWS).

Rocketsonde data collection was conducted onboard USS Lake Erie and radiosonde data was collected onboard USS Lake Erie, USS David R. Ray, and USNS Silas Bent. Figure 5.2 highlights the region of data collection and the general geography and topography of the Persian Gulf and the Gulf of Oman during SHAREM 110. In order to meet thesis objectives, refractivity profiles calculated from radiosondes launched from all three of these platforms as well as rocketsondes launched from the Lake Erie will be examined. The data utilized to contrast propagation loss assessment using RPO was obtained from simultaneously launched rocketsondes and radiosondes. In most cases, the data compared originated from separate

platforms that were in close proximity. Due to the benign nature of the environmental conditions in the Gulf of Oman during this phase of the exercise, the comparison of simultaneously obtained data from separate platforms is feasible and reasonable. However, in a few select cases rocketsondes and radiosondes were launched simultaneously from the USS Lake Erie. Additionally, a few cases of data collection facilitated the analysis of three different simultaneously launched radiosondes in conjunction with a rocketsonde launch. The next chapter will highlight the results of the analysis.

The second phase of SHAREM 110 was conducted from 13 to 17 February 1995 in the Gulf of Oman. This phase represents the time frame for data collected and utilized for analysis in this thesis. During this period, the environmental conditions were not as wide ranging as experienced during the phase conducted from 5 to 12 February 1995 and were considered to be quite benign (Byers 1995). Winds were less than 15 knots and sea/swell heights rarely exceeded 2 ft. Air temperature was in the 20 to 24° C range and sea surface temperatures were almost always between 22 and 23° C. As a result of the sea water being warmer than the air temperature, there was instability in the surface layer. Humidity was generally high at 70 to 80% and in conjunction with low wind conditions, there were highly variable spatial and temporal evaporation ducting conditions. The problem with the evaporation duct calculation is that under certain conditions a one degree change or error in a temperature measurement or a knot change or error in wind speed can cause significant differences in the calculated height. This type of sensitivity requires highly accurate METOC measurements at the ocean surface.

Several significant results were obtained from SHAREM 110 distinctly indicating the

requirement for environmental data that has improved temporal and spatial resolution. The need for continuous measurements is apparent as fluctuations in duct heights can change over short periods of time. While the rocketsonde does not provide continuous environmental data, it is capable of providing requisite updates at time frames far exceeding current MRS data acquisition methods.

The most significant contribution was the successful demonstration of a range dependent EM pathloss model from a shipboard workstation. Using the METOC support system architecture, gridded fields were generated to allow range dependent pathloss calculations utilizing the RPO model. The ability to perform the pathloss calculations and provide the results to SPP-ADM was successfully demonstrated. The RPO application developed for the TESS Remote Work Station (TRWS) on the Lake Erie worked as designed. This represents a significant step forward in the ability to use a range dependent model for shipboard calculation of sensor performance. The results obtained using gridded field data and RPO pathloss appeared to produce general agreement with tactical detection results (PEO USW/ASTO-E 1995). Use of range dependent RPO pathloss appeared, overall, to yield predictions which were more reflective of observed performance than range independent IREPS in most cases. Continued post exercise analysis is required to quantitatively determine the effectiveness of the performance predictions. The integration of the gridded fields and RPO prop loss calculations into SPP-ADM performance prediction functions required significant user interaction. This area is being addressed in future development plans for this system.

Within the SEAWASP system, the ability to generate pathloss values with the

TEMPER propagation model and automatically incorporate them into system performance calculations was demonstrated. The integration of single rocketsonde profiles with evaporation duct data into the SEAWASP workstation, where TEMPER and the SPY-1B performance model subsequently made use of the data, required very little user interaction. Between rocketsonde launches, 5 minute updates to the SPY-1B performance estimates using sensor pole data occurred automatically. Overall, using a single rocketsonde profile, the SEAWASP system appeared to produce excellent agreement of within 15% between predicted and observed SPY-1B firm track range for the majority of low-altitude track events when the environment was adequately characterized (PEO USW/ASTO-E 1995).

Detailed analysis of the environmental data should address identification of critical METOC parameters affecting radar prediction, the temporal/spatial nature of those parameters in the littoral areas, and in particular, the validity of the measured refractivity with the use of ship launched minirawinsondes using current initializing METOC data. In any case the SHAREM conclusively showed the significance of accurate environmental data and the complexity involved in obtaining such data. The SHAREM 110 Quicklook (PEO USW/ASTO-E 1995) recommended that all rawinsonde data should be stored as high resolution vertical profiles. The next section will take a close look at the rocketsonde and radiosonde data obtained during the exercise and will show the significant differences in calculated propagation loss between the two types of available data. The propagation loss calculations will show RPO's sensitivity to accurate and more vertically resolved data. The use of RPO onboard ships at-sea has been successfully demonstrated and will represent the wave of future development of shipboard propagation assessment. It only follows that

improved data collection will be required to support the RPO model and the rocketsonde represents a sound and reliable source of high vertical resolution data. Other methods of obtaining higher vertically resolved data are under consideration such as the Tactical Dropsonde (TDROP) and the Deck Launched Sonde (DELS) that would also represent excellent data sources for the range dependent propagation loss model expected to be implemented in shipboard tactical decision aids such as TESS and SPP-ADM.

VI. DATA COMPARISON

Twenty eight rocketsondes were launched during SHAREM 110 (5 to 17 February 1995). Twelve of these were launched during the second half from 13 to 18 February 1995 in the Gulf of Oman (GOO). The latter data were the most extensively reviewed. Two rocketsonde launches conducted on 09 February 1995 in conjunction with radiosonde launches revealed interesting comparisons and were evaluated. A 24 h period from 0300Z 16 February 1995 to 0300Z 17 February 1995 provided a unique evaluation of radiosonde/rocketsonde data through a quickly developing synoptic weather phenomena known as a Short Shamal event (Byers 1995). In addition, a simultaneous launch of a rocketsonde and radiosonde was conducted onboard the USS Kitty Hawk on 21 January 1994 in the Southern California (SOCAL) operating area. This represented the first operational launch and use of a rocketsonde onboard a U.S. Navy aircraft carrier. Previously, all rocketsonde launches had been conducted onboard Aegis class cruisers by the Johns Hopkins University Applied Physics Lab in support of Aegis system development and evaluations.

An important consideration in selecting rocketsonde launches for this study was that the RPO propagation loss model requires the "0" level, (i.e. atmospheric parameters of temperature, humidity, and pressure at the surface). Since one of the rocketsonde's major contribution is the surface level data, it was critical to only evaluate those rocketsonde soundings that contained the surface data. Only three of the rocketsondes launched failed to yield surface data. The lack of data acquisition at the surface for these three rocketsonde

soundings was not determined.

The balloon launched radiosondes obtained during SHAREM 110, as well as all radiosonde data in general, indicate a distinct lack of surface data. This lack of surface data can range anywhere from 25 to 30 ft for soundings that were conducted onboard the USS Lake Erie to 60 ft for the sounding that was obtained from the USS Kitty Hawk. Figure 6.1 represents modified refractivity versus altitude profiles for radiosondes launched from the USS Lake Erie and USS Kitty Hawk respectively. Note the gap or lack of data from 10 m to the surface for the USS Lake Erie sounding and from 20 m to the surface for the USS Kitty Hawk. Ultimately, the use of balloon launched radiosondes greatly degrades the effectiveness of range dependent propagation loss models such as RPO because the model will not run without the surface data.

For this study, and also if balloon launched radiosondes were to be used in the shipboard environment in conjunction with RPO, it would require some form of surface data interpolation in order for the model to have the requisite surface sounding to calculate propagation loss. The radiosonde data evaluated with RPO in this study were modified so that they would be accepted by the RPO model and thus could be compared to the outputs obtained from the rocketsonde data. The radiosonde data was artificially induced with surface layer data by utilizing the gradient established between the first two data points of the sounding and extending this gradient to the surface. In many cases extension of this gradient to the surface was not an accurate reflection of the actual M unit profile as Figures 6.2a and 6.2b highlight. Figure 6.2a is the USNS Silas Bent radiosonde launched at 1200Z on 11 February 1995 with the gradient between the first two M units extended to the surface. Figure

6.2b is the USS Lake Erie rocketsonde from 1200Z on 11 February 1995 with measured data to the surface. Note the significant difference between the two soundings. The USNS Silas Bent profile indicates near standard refractive conditions whereas the USS Lake Erie profile reveals a decrease in M units which is indicative of a trapping layer near the surface and several thin layers between 50 and 80 m. Of the 14 rocketsonde launches from 8 to 17 February 1995, 6 were conducted in conjunction with balloon launched radiosondes from the USNS Silas Bent. In general, the distance separating the radiosonde launches and the rocketsonde launches onboard the USS Lake Erie was less than 20 miles. There was only one instance where the distance between these two units was greater than 20 miles. This occurred on 15 February 1995 where the distance between these two units approached 35 miles. In any case, the meteorological conditions throughout the area would indicate that similar refractive conditions were present over the area during this time frame.

The Shamal condition persisted in the Persian Gulf throughout the first half of SHAREM 110. It lasted from approximately 00Z 9 February to about 03Z 14 February (after Byers 1995). The Shamal condition is indicative of dry, offshore winds that leads to a strong moisture gradient in the vertical.

The rocketsonde and radiosonde soundings for 1800Z 09 February, 1200Z 11 February, and 0300Z 13 February when analyzed in conjunction with the synoptic situation reveal significant differences. Figures 6.3 - 6.5 represent the M unit versus altitude profiles for the radiosonde and rocketsonde soundings taken from the USNS Silas Bent and USS Lake Erie, respectively. The 1800Z 09 February 1995 USS Lake Erie rocketsonde (Figure 6.3) certainly displays multiple layers below 150 m , a non-uniform M profile. The 1200Z 11

February and 0300Z 13 February 1995 Lake Erie rocketsondes (Figures. 6.4 and 6.5) show low-level trapping that is not found in the radiosonde profiles. The most dramatic example of the variation between radiosonde and rocketsonde refractive profiles is presented in Figure 6.3. Figure 6.3a represents the plot of temperature (Ta) in red and dew point (Td) in blue in °C. The Ta and the Td are significantly different between the two soundings. The Td for both soundings start at very similar temperatures however, the rocketsonde Td is highly variable and shows several regions of drying accounting for the enhanced refractive conditions. The temperatures are in closer agreement between the two soundings but do show some variation. The radiosonde temperature profile shows a slight increase in temperature up to 75 m then a gradual decrease. The rocketsonde profile shows a slight gradual decrease from the surface to approximately 250 m followed by a gradual temperature increase.

The radiosonde launched from the USNS Silas Bent revealed nearly standard refractive conditions through 300 m. In contrast, the rocketsonde which provided a much finer vertical resolution of the data revealed significant variations in the refractive profile from the surface to 300 m. These two soundings were conducted within approximately 12 miles of each other yet yield significantly different refractive conditions. The profiles examine in particular the lower levels to 300 m. This scale assists in illustrating the significant difference in refractive profiles that are obtained via the different sounding methods. The three radiosonde soundings conducted on the USNS Silas Bent represent standard refractive conditions whereas the rocketsonde soundings taken onboard the USS Lake Erie are indicative of and support surface based ducting.

Figures 6.6-6.11 represent the propagation loss for these radiosonde and rocketsonde

soundings computed by RPO version 1.15 that would be expected for a generic SPS-10 surface-based surface search radar typically found onboard U.S. Navy ships. The propagation loss curves supported by the radiosondes (Figures 6.6 - 6.8) all reveal near standard propagation conditions whereas the rocketsonde based propagation loss curves (Figures 6.9 - 6.11) all support the surface based ducting conditions as expected and dictated by the synoptic situation. Of particular interest is RPO's sensitive response to the fine scale resolution depicted by the rocketsonde. The various small scale trapping layers in the rocketsonde sounding are evident by the extended propagation revealed in Figure 6.9 at various levels above the surface.

To further illustrate the variability obtained in soundings, it is interesting to look at additional M unit profiles and associated RPO outputs from simultaneously launched radiosondes and rocketsondes from the USS Lake Erie. The rocketsonde and radiosonde data was simultaneously collected from the USS Lake Erie located in the GOO on 16-17 February 1995. During this period, the synoptic situation was characterized by southeasterly winds known as Kaus winds. Kaus winds generally precede a short and generally weaker Shamal event. This type of short Shamal event typically lasts 24 to 36 h. Shamal conditions produced northerly offshore flow resulting in the formation of a shallow boundary layer topped by dry air and a slight inversion. This led to a trapping layer and produced ducts ranging from slightly elevated to surface based. Typically, the ducting conditions during this short Shamal period are present but are characteristically weaker.

Figures 6.12 - 6.15 represent the M unit profiles for the radiosondes and rocketsondes conducted on the USS Lake Erie during this short Shamal period. The soundings were taken

at 0300Z, 0900Z, and 1500Z on 16 February, and 0300Z on 17 February. There were two balloon launched radiosondes taken at 0300Z on both 16 and 17 February.

This 24 h case is interesting because the profiles evolve through cases that are important, as discussed. With pre-Shamal (Kaus) conditions, Figure 6.12, the rocketsonde profile is near-normal below 300m. Temperature and dew point profiles (Figure 6.12a) suggest an elevated trapping layer exists between 300 and 600 m. With the beginning of Shamal, Figures 6.13 and 6.14, elevated trapping continues. Finally, with full intensity of Shamal, Figure 6.15, a near-surface duct appears in the rocketsonde.

Even the differences between the balloon launched radiosondes taken from the USS Lake Erie yield significantly different results. Figure 6.12a represents the Td and Ta profiles for the two radiosondes conducted and the rocketsonde conducted at 0300Z 16 February onboard the USS Lake Erie. The first radiosonde and the rocketsonde Td and Ta profiles are closely matched however, the lowest level of the profiles below 100 m reveal differences in the Td and Ta that can be attributed to ship influences. Overall, there is a disparity in the lower levels between the Td and Ta profiles obtained from the radiosonde and rocketsonde, respectively. In particular, both radiosonde Td and Ta profiles (Figure 6.12a) show a drier atmosphere below 200 m compared to the rocketsonde. Further illustration is provided in Figure 6.14a that shows the Td and Ta profiles for the radiosonde and rocketsonde conducted 1500Z 16 February 1995. Note the close proximity between the first data points for both Td and Ta for the two soundings. Following initial agreement, the radiosonde shows a rapid decrease in Td up to 375 m whereas the rocketsonde reveals a much smoother and less rapid decrease in Td up to 250 m. Both of these soundings yield surface ducting conditions but, the

ducting revealed by the radiosonde data reaches 200 m whereas the ducting measured by the rocketsonde only reaches heights of approximately 20 m. This determination of duct height will impact expected detection ranges which will be discussed.

The M unit versus altitude profiles for the two radiosondes and rocketsonde conducted at 0300Z 17 February 1995 (Figure 6.15) correspond to the period of full intensity of the short Shamal event. All three M unit versus altitude profiles in Figure 6.15 reveal some form of near surface trapping as expected. However, the most intense surface trapping is indicated by the rocketsonde as illustrated by the propagation loss curve in Figure 6.25.

The propagation loss curves for each of these M unit profiles is provided in Figures 6.16 - 6.25. It is evident from figures 6.16 and 6.17 which represent the two radiosonde profiles from 0300Z on 16 February, and Figures 6.23 and 6.24 which represent the two radiosonde profiles from 0300Z 17 February that even radiosondes launched from the same platform within minutes will yield significantly different results. The variations can be attributed to shipboard effluence and different initial surface data. To illustrate the impact of the initial surface data consider the initial data for the two radiosondes and the rocketsonde from 0300Z on 16 February 1995 presented in Table 6.

LAKE ERIE Type	Height (m)	Temp C	Dew Point Depression C	Pressure (mb)	Location
Radiosonde	6.0	23.0	9.5	1017.0	25.14 N 058.61E
Radiosonde	6.0	24.0	12.0	1015.5	25.09 N 058.71 E
Rocketsonde	0	22.3	7.2	1015.1	25.11 N 058.61 E

Table 6. Variations in Initial Surface Data

There is a significant disparity in the initial surface data between the two radiosondes which should have basically the same values considering their close proximity. The radiosondes may be affected by the input of erroneous surface data. This is not a factor for rocketsondes as the surface data is a measured quantity and thus the opportunity for human error is eliminated. In any case, use of these propagation loss calculations would certainly yield significantly different detection ranges for a particular radar.

To further describe the different results obtained from rocketsondes and radiosondes, the RPO outputs from the soundings conducted at 1500Z on 16 February 1995 onboard the USS Lake Erie were used with Engineer's Refractive Effects Prediction System (EREPS). EREPS is a system of individual stand-alone IBM/PC-compatible programs designed to assist an engineer in properly assessing electromagnetic propagation effects of the lower atmosphere on proposed radar, electronic warfare, and communication systems. The executable program within EREPS utilized for this analysis was PROPR. PROPR generates a graphic display of propagation-loss versus range under measured environmental conditions relative to a specified threshold. The threshold establishes the required dB level for detection. The

threshold is based on a user-defined radar cross section and probability of detection. The user can asses a radar's maximum expected detection range by identifying where the propagation loss intersects the threshold of detection. Free space propagation is defined as propagation in a region whose properties are isotropic, homogeneous, and loss-free, i.e. away from the influences of the earth's atmosphere. This analysis was done to assess the expected detection range for an SPS-10 radar against a one square meter target with a 90 percent probability of detection. The target height was established at 60 ft and the receiver height was established at 82 ft. The results, illustrated in Figures 6.26 and 6.27, reveal the significant differences in associated propagation loss as well as expected detection ranges. The propagation in Figure 6.26 (from the radiosonde) reveals an extended multipath propagation with potential detection in excess of 60 nm with maximum continuous detection expected to approximately 25 nm. This is because both the target and receiver are located within the assessed surface based duct height of approximately 200 m. It is highly unlikely that the SPS-10 surface search radar would be capable of detecting a 1 square meter target at 90 percent probability of detection unless extremely strong surface based ducting conditions were present. The rocketsonde data derived propagation loss profile in Figure 6.27 more closely resembles the expected detection with maximum continuous detection approximating 16 nm. The M unit profile showed slight surface ducting conditions to approximately 20 m. For this scenario both the target and receiver are located above the measured surface duct of 20 m. Thus, there is no indication of extended propagation from the propagation loss display as would be expected considering the meteorological conditions.

Another interesting case is revealed from the sounding data obtained on 13 February

1995. Comparison of data obtained from two balloon launched radiosondes onboard the USS Lake Erie, one radiosonde from USNS Silas Bent, one radiosonde from USS David R. Ray, and a rocketsonde conducted at 1200Z reveal significantly different M unit profiles and propagation loss results. This time frame marked the beginning of the second half of SHAREM 110 with operations conducted in the GOO. The synoptic situation was characterized by a weakening Shamal condition with characteristic transition to Northeast monsoonal flow. By approximately 0300Z 13 February 1995 the Shamal had weakened and the transition to the Northeast Monsoon was in effect. The true monsoonal flow had reestablished itself by 0000Z 14 February 1995.

Analysis of the M unit profiles as well as the associated RPO propagation loss model runs reveal some form of surface based trapping in all balloon launched radiosondes while the rocketsonde indicates fairly normal conditions. Figures 6.28 - 6.30 are the M unit profiles from 1200Z on 13 February 1995. Figure 6.28 represents the two radiosonde profiles launched from the USS Lake Erie. Figure 6.29 represents the radiosondes launched from the USS David R. Ray and USNS Silas Bent respectively. Figure 6.30 is the rocketsonde launched onboard the USS Lake Erie. Table 7 illustrates the wide variety of initial surface data utilized for M unit profiles as well as RPO propagation loss model outputs, and represent a reasonable explanation for the significant differences and wide variety of related propagation loss predictions as illustrated in Figures 6.31 - 6.35.

Type	Height (m)	Temperature C	Dew Point Depression C	Pressure (mb)	Location
Radiosonde USS Lake Erie A	6.0	26	11.2	1012.0	26.64N 057.31E
Radiosonde USS Lake Erie B	6.0	26	11.2	1012.0	25.54N 057.69E
Radiosonde USS David R. Ray	0.7	23	6.0	1015.0	24.71N 057.31E
Radiosonde USNS Silas Bent	6.0	24	12.0	1013.9	25.29 N 057.56E
Rocketsonde USS Lake Erie	0.0	22	8.9	1014.0	24.77N 057.62E

Table 7. Variations in Initial Surface Data for 1200Z Soundings on 13 February 1995. Location varied with ship movement.

The important feature in the radiosonde obtained data is the surface-based ducting conditions. It is believed that this is wrong and due to heated ship effect as shown in Table 7. Figures 6.30a and 6.30b are the Td and Ta profiles for radiosondes and the rocketsonde. The two radiosondes launched from the USS Lake Erie as well as the radiosonde launched from the USNS Silas Bent show a rapid decrease in temperature below 100 m. The temperatures measured from the USS David R. Ray radiosonde and the rocketsonde launched from USS Lake Erie are very similar yielding slight decreases in temperature with height. The Td plots also reveal interesting contrasts. The four MRS radiosonde obtained soundings reveal rapid decrease in Td below 100 m whereas the rocketsonde reveals a relatively constant Td with height below 100 m.

Figures 6.31 and 6.32 represent the RPO based propagation loss curves for the

radiosondes launched onboard the USS Lake Erie at 1200Z 13 February 1995. Both soundings highlight the surface based ducting as evidenced by the extended ranges near the surface. The second sounding, however, reveals far less extended propagation than the first sounding. The propagation loss as described by the radiosonde profiles launched from the USS David R. Ray and USNS Silas Bent and illustrated in Figures 6.33 and 6.34 show strong surface based ducting conditions and reflect very minimal propagation loss. It is highly suspect that these conditions were present as the onslaught of the Northeast monsoonal conditions would be more supportive of normal refractive conditions. The case for normal refraction is most closely supported by the rocketsonde profile as evidenced by the propagation loss diagram in Figure 6.35. This form of propagation loss would be the most representative of the five cases as supported by the synoptic meteorological conditions. Once again an argument can be made for variance in initial surface data as well as other compounding issues such as ship effluence and increased vertical resolution that attribute to variations and errors in balloon launched radiosondes. The rocketsonde which eliminates these potential hazards and errors provides the most accurate representation of the environment and conclusively supports the actual environmental conditions. This type of high resolution data will provide the range dependent propagation loss model that supports sensor performance prediction the requisite input to most accurately support the tactical decision makers.

A final analysis was conducted with data obtained from a simultaneously launched radiosonde and rocketsonde from the USS Kitty Hawk (CV 63) on 21 January 1994. This represented the first rocketsonde launch from an aircraft carrier and convincingly proved its ease of operation and its potential for valued use onboard a Navy vessel that maintains an

enormously high tempo of aircraft operations. During the launch the synoptic meteorological situation off the coast of southern California was dominated by offshore flow produced by the Santa Ana condition. Like the Shamal, the Santa Ana's offshore flow typically produces enhanced refraction resulting from an elevated trapping layer and surface based ducting.

Figure 6.36 illustrates the M unit profiles obtained from the simultaneous launched radiosonde and rocketsonde. Analysis of both the radiosonde and rocketsonde data support the identification of the surface based duct feature. However, there are some significant differences in the M unit profiles. First, and probably most significantly is the lack of data from 20 m to the surface on the radiosonde sounding. This requires that some form of data interpolation be used to fill in the void of data at the surface in order to run the RPO propagation loss model. This interpolation, in conjunction with the potential error in the initial surface data utilized in the MRS, could compound the error. The point illustrated here is that there is a much larger margin for error when involved with a large deck ship such as an aircraft carrier whose balloon launched radiosondes are typically released from 20 to 30 m above the waterline. There is, however, data available from 20 m to the surface as noted on the rocketsonde sounding in Figure 6.36, which avoids the complications and potential errors involved with data interpolation and initial surface conditions as raw data is collected all the way to the water's surface.

Figure 6.36 highlights the structure of the M unit gradient as it is depicted in the radiosonde and rocketsonde profile. Note the much sharper gradient in M units at approximately 250 m on the radiosonde profile. This is caused by the radiosonde measurements indicating drier air above the inversion. Figure 6.36a shows the Td and Ta

versus altitude plot for the radiosonde and rocketsonde. Note that just above the inversion the Td was approximately -10° C for the radiosonde versus -5°C for the rocketsonde. The reason for this difference can't be explained by resolution or the down versus up sonde traverse.

Lastly, the aircraft carrier induces such a large wake of contamination that the temperature field surrounding the ship can be as much as 3° C higher than the temperature outside of the ship's influence. This contaminated temperature field measured by the balloon launched radiosonde can affect the sounding up to as much as 1500 ft (John Rowland, personal communication, 1996). For the soundings conducted onboard the USS Kitty Hawk the variations in the Td and Ta profiles near the surface highlight the effect of ship influences. The major difference in the profiles above the inversion is due to the variability in the measured Td. These soundings yielded similar RPO propagation loss profiles as expected primarily due to the strength of the elevated trapping layer and associated surface based duct. The height of contamination will vary depending on various conditions and shipboard operations but undoubtedly some form of contamination will be present that will alter the temperature field. Figure 6.37 illustrates the significant temperature differences, particularly below the inversion, obtained from the radiosonde and the rocketsonde. Note that once the radiosonde reaches an altitude of approximately 600 m the temperatures between the two soundings are in closer agreement and to within approximately 1 degree C.

VII. CONCLUSION AND RECOMMENDATIONS

This thesis investigated the reasons for the variability in predicted atmospheric refraction. Its main focus was the comparison of refractive profiles from balloon launched radiosondes and rocketsondes. The sounding data were obtained during simultaneous launches from U.S. Navy ships operating in the Persian Gulf and Gulf of Oman during SHAREM 110 conducted from 05 to 17 February 1995. Comparison of the two types of data often yielded significantly different M unit profiles and subsequently resulted in uniquely different propagation loss calculations as performed by RPO.

This study has shown the distinct need for fine scale vertical profiles with resolution approaching 5 m. The use of the MRS onboard U.S. Navy ships by either Mobile Environmental Teams or OA divisions distinctly lacks the vertical resolution necessary to accurately classify the refractive conditions. The vertical resolution obtained from balloon launched radiosondes used in conjunction with the MRS can approach 20 m which does not satisfactorily sample the environment to provide a representative description of the refractive conditions. The MRS would require modification to the data processing capability to provide the higher resolution data that the sonde is capable of measuring. The rocketsonde is recommended because of its unique ability to provide high resolution data.

The lack of data at or near the surface also impacts the balloon launched radiosonde's ability to accurately depict the environment. The shipboard launched radiosondes are typically launched anywhere from 10 to 20 m above the waterline. RPO requires initial surface data to calculate propagation loss. Thus, the only way to utilize radiosonde data with RPO is to

estimate the surface data values of temperature, pressure, and humidity. This is often done, as was the case in this study, by interpolating the surface data by extending the gradient of modified refractivity between the first two data points to the surface. In conjunction with initial surface data, this study highlighted the potential errors that may be induced in the refractive profiles by inaccurate initial data inputs to the MRS. Since this data is typically obtained via observation from shipboard measurement systems (i.e. barometer/thermometer located on bridge) the margin for error can be tremendous. The rocketsonde is recommended for use because it eliminates the need for estimating the surface data as it continuously samples the environment from its peak altitude until it reaches the surface.

The rocketsonde's most significant contribution seems to be its ability to measure environmental data away from the ship's influence. Studies have revealed that contamination from the ship impacts the accuracy of radiosonde particularly at lower altitudes. Temperature, for example, measured onboard ship may be as much as 2-3° C higher as a result of radiation influences and heat generated by the ship. Ensuring that the radiosonde is properly acclimated prior to launch is also a major factor. In order to ensure proper sensor acclimation, sufficient airflow through the sensors must be obtained. This clean flow of air through the sensors is only obtained after the sonde is sufficiently far enough away from the ship's influence. This adjustment period jeopardizes the accuracy of the radiosondes initial measurements. The rocketsonde also requires proper acclimation but the key point is that the acclimation is done away from shipboard influences and is completed prior to reaching the lowest levels where the critical surface data and lower level environmental conditions are measured.

The rocketsonde is capable of providing upper air sounding data in environments that

are too harsh to successfully release a balloon launched radiosonde. High winds and sea states will not affect the ability to launch a rocketsonde. The rocketsonde can obtain the requisite environmental parameters for refractive assessment in less than half the time required to prepare and launch a balloon guided radiosonde. The rocketsonde requires no specific ship maneuvering requirements as the rocketsonde is not impacted by the relative wind direction or speed. Lastly, for MET deployments it will eliminate the need to transport and store helium bottles which are cumbersome and require replenishment at sea.

With the incorporation of the range dependent propagation loss model RPO in shipboard sensor performance prediction systems such as TESS, it becomes increasingly more important that better environmental data be obtained and utilized. Better environmental data incorporates the concepts of both increased vertical resolution as well as being obtained away from the ship's influences. The radiosonde does sample the environment at higher intervals than that which is provided by the MRS, yet the other significant factors previously discussed reduces it's effectiveness as an environmental sounding instrument.

Several methods of obtaining the environmental parameters required to determine the refractive conditions are currently being investigated. Light Detection and Ranging (Lidar), the Tactical Dropsonde (TDROP), and the Deck Launched Sonde (DELS) are technologies that are being looked at and developed with the intention of providing suitable environmental data to meet the Navy's need for high resolution data. The DELS, for example, uses an unmodified Tactical Drop Sonde propelled by a rocket motor launched from the chaff dispenser installed onboard most U.S. Navy ships. These methods are still being developed and could be several years away from implementation. The rocketsonde system provides

ready-made, off-the-shelf technology that is capable of providing high resolution data from 10,000 ft to the surface and away from shipboard influences.

The rocketsonde represents the quickest means of improving EM/EO performance prediction capabilities through exploitation of currently developed technology. Currently, the rocketsonde has been developed to reach altitudes of 10,000 ft and contains GPS wind finding technology. Development of the rocketsonde system continues and it is expected that within the next year the rocketsonde will be capable of reaching a peak altitude of 20,000 - 30,000 ft. When this altitude is reached, consideration could be made to permanently replace the balloon launched radiosonde with the rocketsonde onboard ships at-sea.

The tactical decision making personnel of today's Navy rely more and more on computer based technology. The ability to use this computing power to accurately model the environment in an attempt to optimize sensor utilization and performance is the ultimate goal. The U.S. Navy's use of balloon launched radiosondes to collect data for use in performance predictions related to radar propagation is not satisfactory in providing the warfare commander with the accurate sensor performance assessment he requires to make sound tactical decisions and plans. The rocketsonde system provides the requisite environmental data to support the most accurate representation of the environment particularly at lower altitudes.

Figure 2.1 Rocketsonde in launcher (after Rowland and Babin 1987).

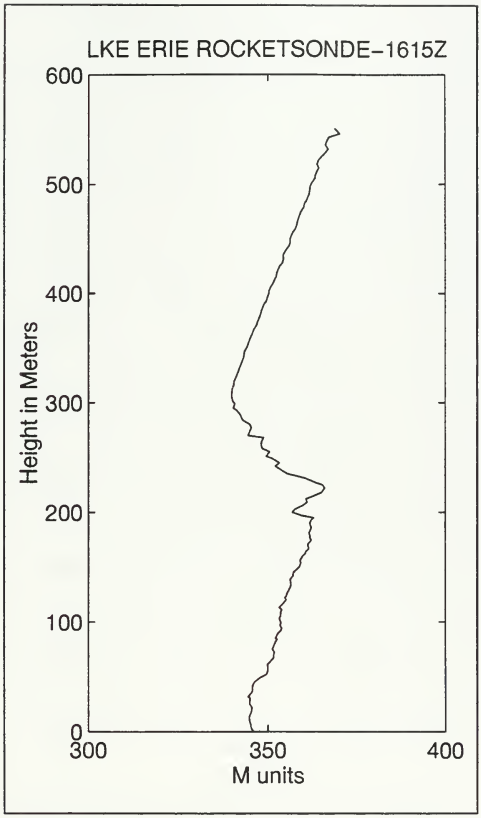

Figure 2.2 Fine-scale modified refractivity profile obtained with rocketsonde launched from operational U.S.Navy ship.

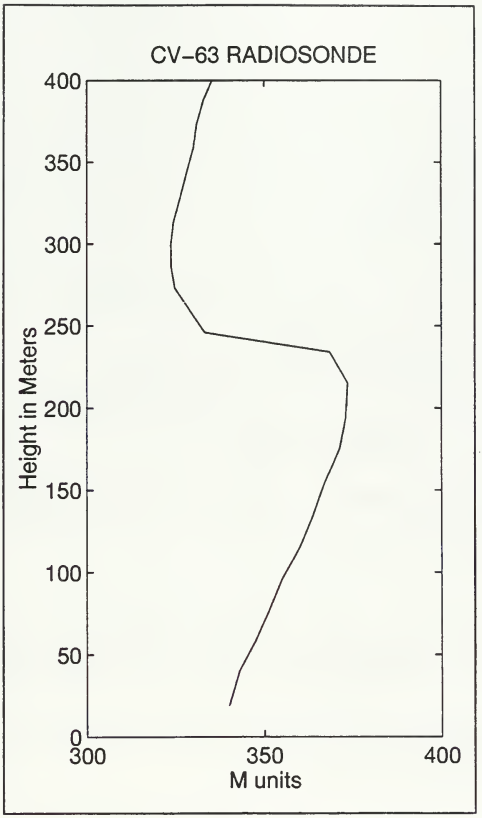

Figure 2.3 Coarse modified refractivity profile obtained with balloon launched radiosonde from operational U.S. Navy ship.

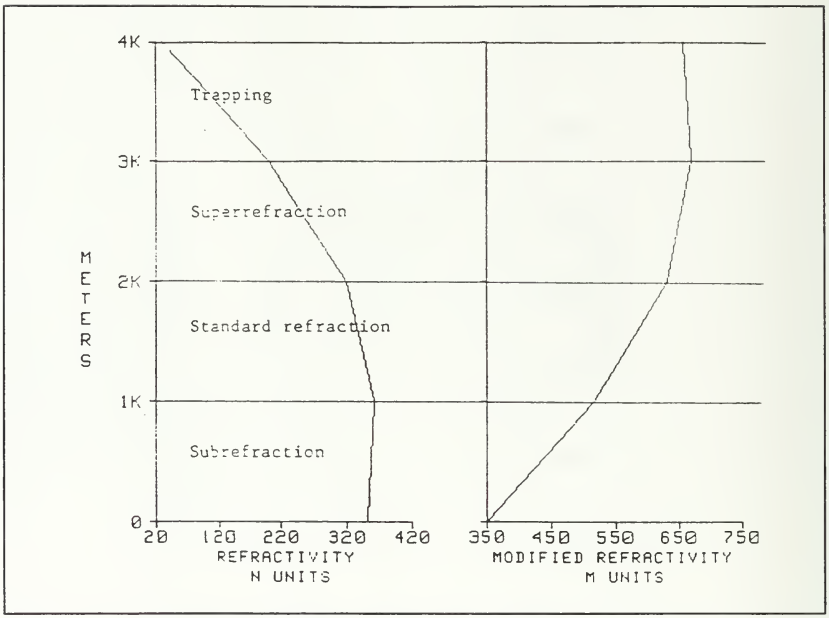

Figure 3.1 Refractivity N and modified refractivity M versus altitude for various refractive conditions (after Patterson 1988).

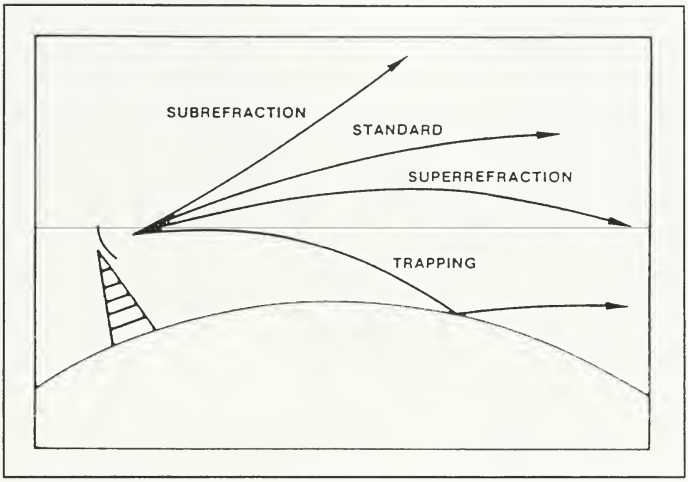

Figure 3.2 Wave paths for various refractive conditions (after Patterson 1988).

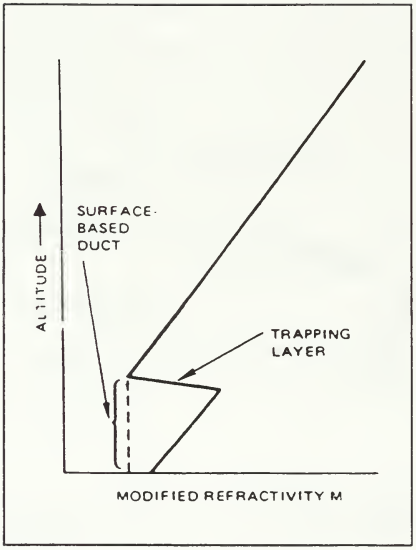

Figure 3.3 Modified refractivity versus altitude for a surface-based duct (after Patterson 1988).

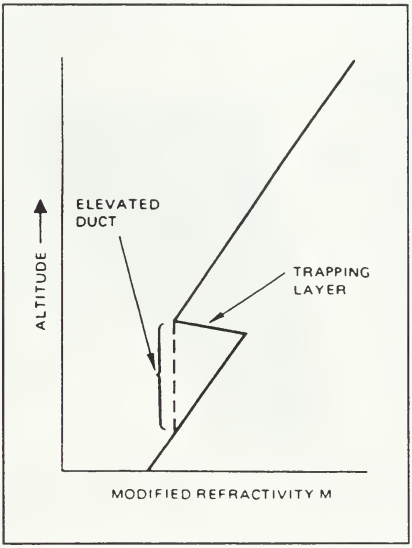

Figure 3.4 Modified refractivity versus altitude for an elevated duct (after Patterson 1988).

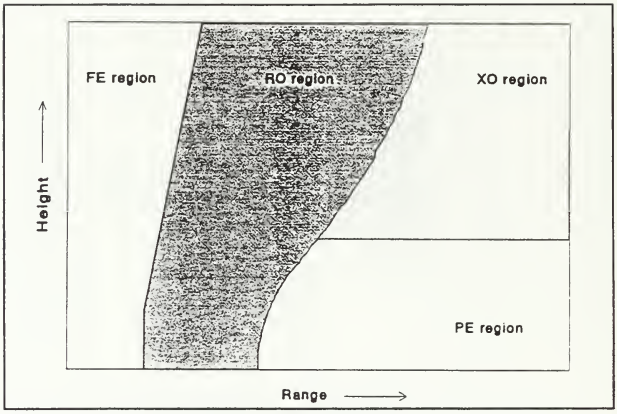

Figure 4.1 RPO calculation regions (after Patterson and Hitney 1992).

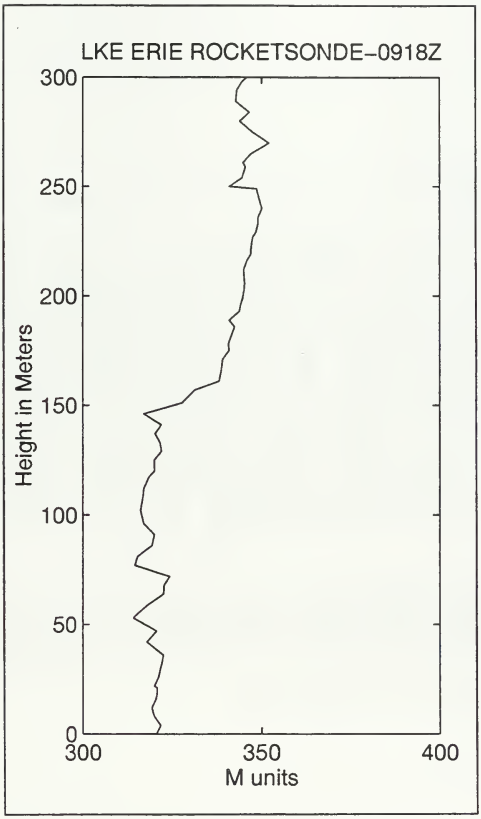

Figure 4.2 Modified refractivity profile highlighting improved vertical resolution obtained via rocketsonde.

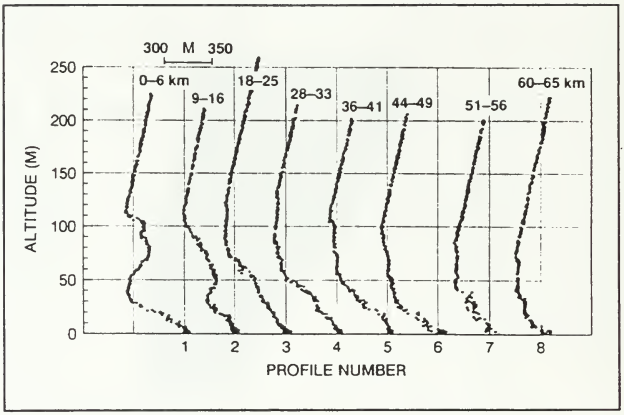

Figure 4.3 Refractivity profiles collected with instrumented helicopter near San Nicolas Island, California on 19 March 1988. The modified refractivity scale for the first profile is shown (after Dockery and Goldhirsh 1994).

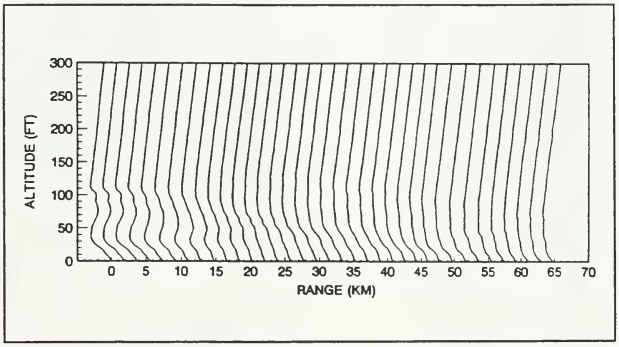

Figure 4.4 The smoothed and interpolated San Nicolas Island refractivity data after processing by LARRI (after Dockery and Goldhirsh 1994).

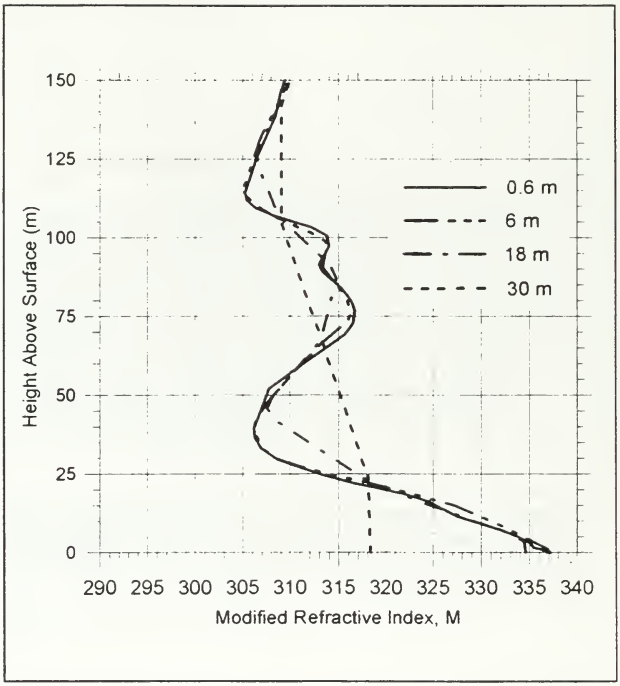

Figure 4.5 Original and reduced resolution of profile 1 from Figure 3.3 after LARRI processing (after Dockery and Goldhirsh 1994).

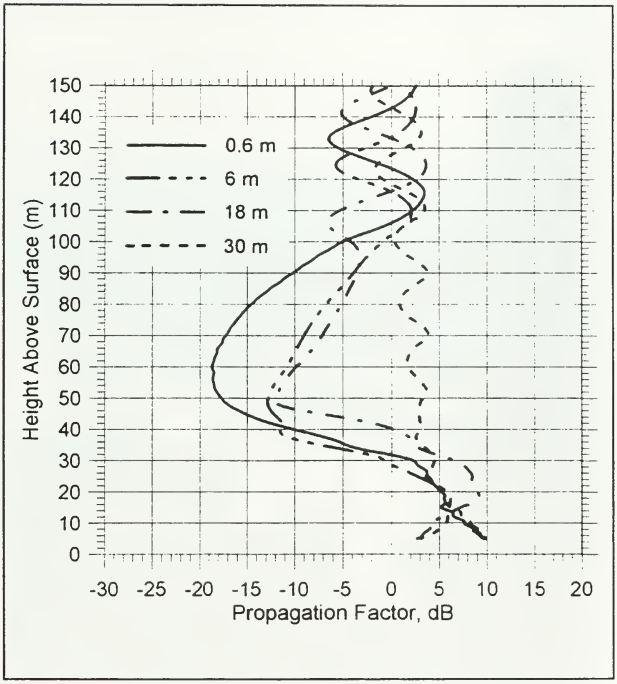

Figure 4.6 TEMPER propagation factor calculations for 10 Ghz at 30 km using the San Nicolas profiles of Figure 3.5 (after Dockery and Goldhirsh 1994).

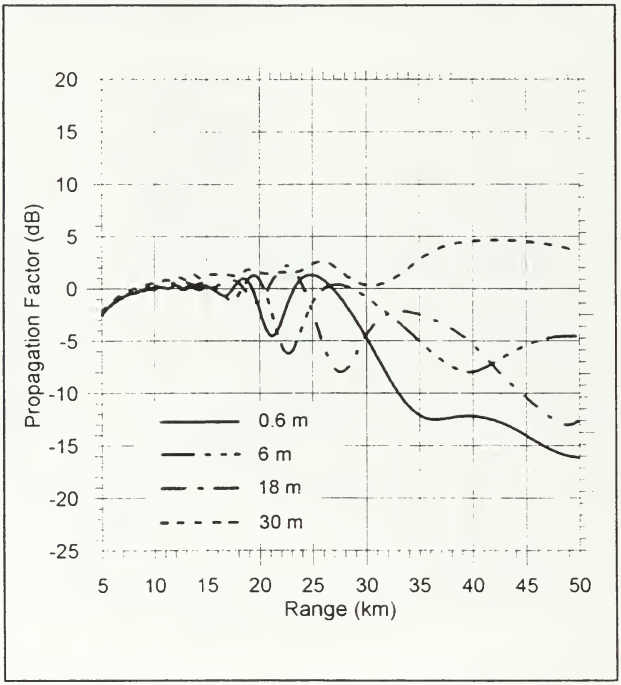

Figure 4.7 10 Ghz propagation factor calculations at 100 m altitude using the San Nicolas profiles of Figure 3.5 (after Dockery and Goldhirsh 1994).

Figure 4.8 Rocketsonde assembly in launcher and data acquisition computer during launch (U.S. Navy photo).

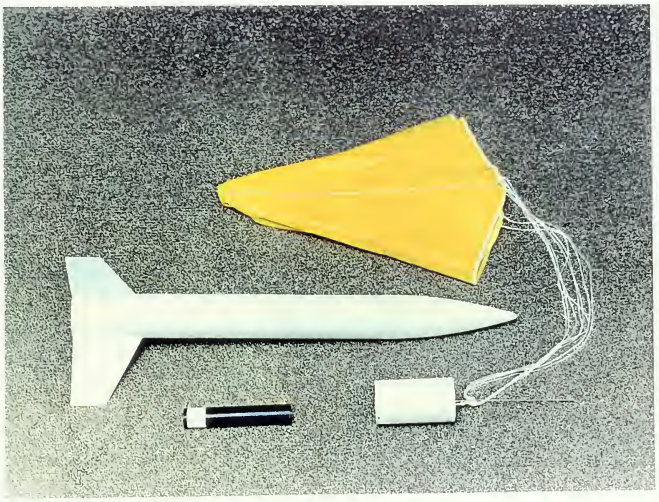

Figure 4.9 Component parts of the rocketsonde including the rocket body, nose cone, engine, and instrument package attached to a parachute (after Rowland and Babin 1987).

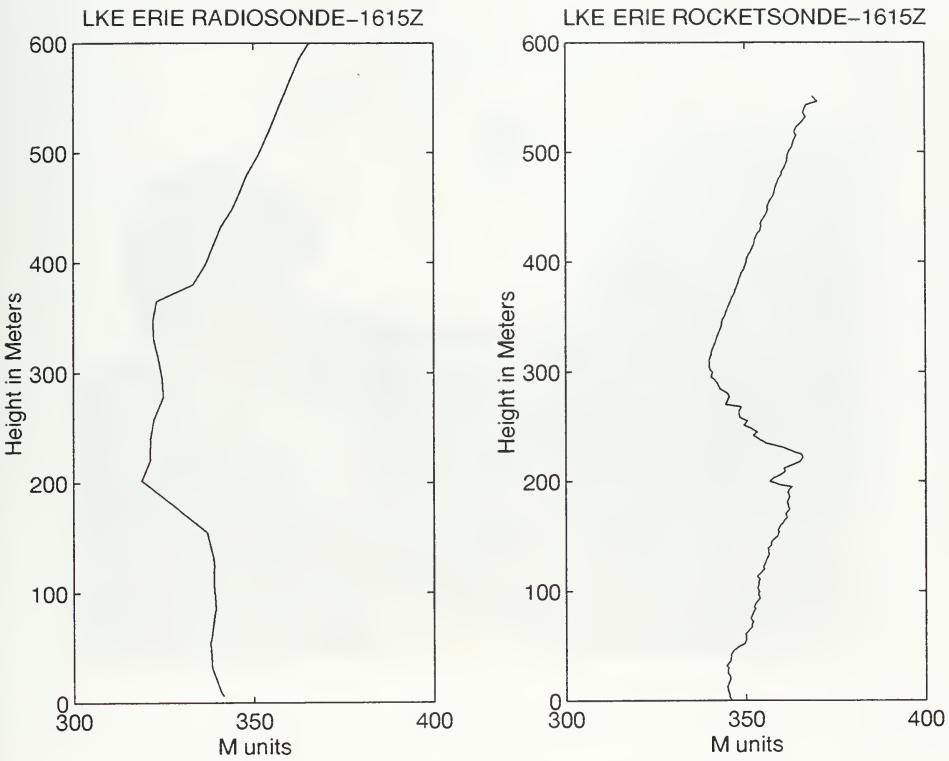

Figure 4.10 Illustration of the significant difference in vertical resolution of M unit profiles from a simultaneously launched radiosonde and rocketsonde at 1500Z 16 February 1995 during SHAREM 110.

Figure 4.11 The MARWIN MW 12 Rawinsonde Set (MRS).

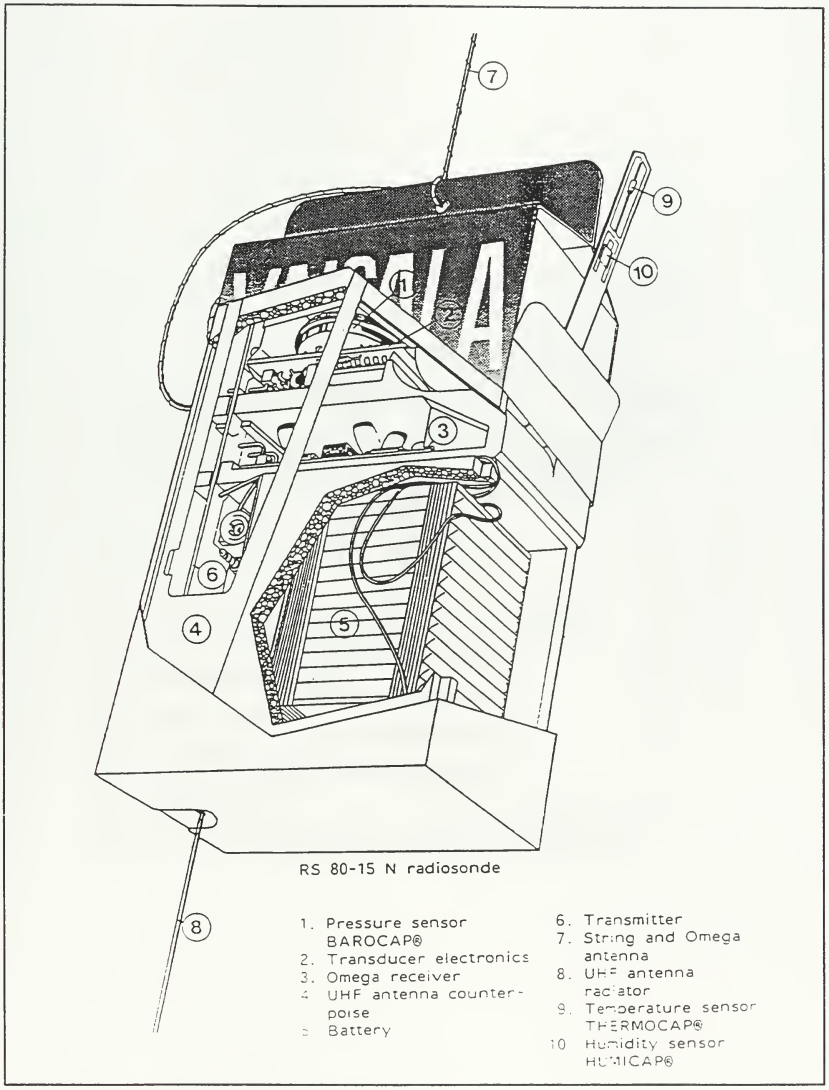

Figure 4.12 The RS 80 - 15N radiosonde.

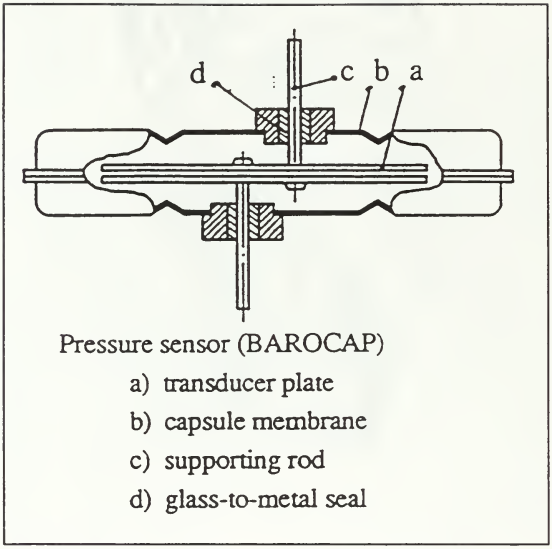

Figure 4.13 The BAROCAP pressure sensor.

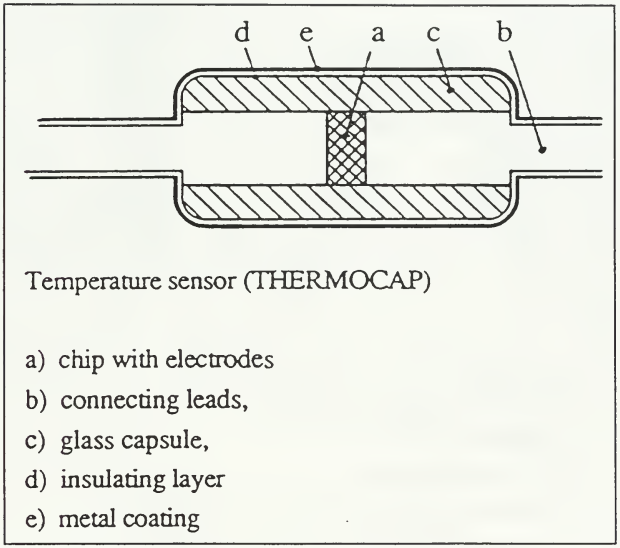

Figure 4.14 The THERMOCAP temperature sensor.

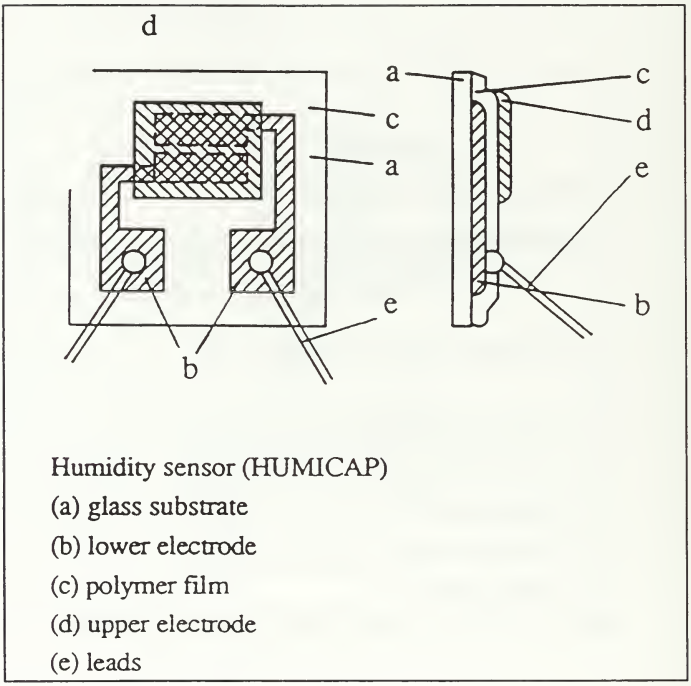

Figure 4.15 The HUMICAP humidity sensor.

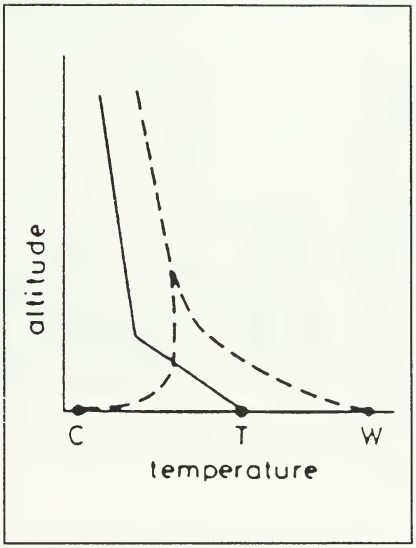

Figure 4.16a Idealised daytime temperature profile with superadiabatic surface layer. Hygristor temperature curves for initially warm (W) and cool (C) sensor (after Helvey 1983).

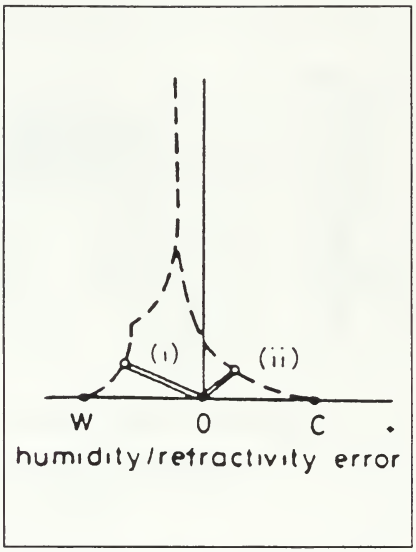

Figure 4.16b Corresponding daytime humidity/refractive error profiles. (I)Apparent super-refractive layer: initially warm hygristor (ii)Apparent subrefractive layer : initially cool hygristor (after Helvey 1983)

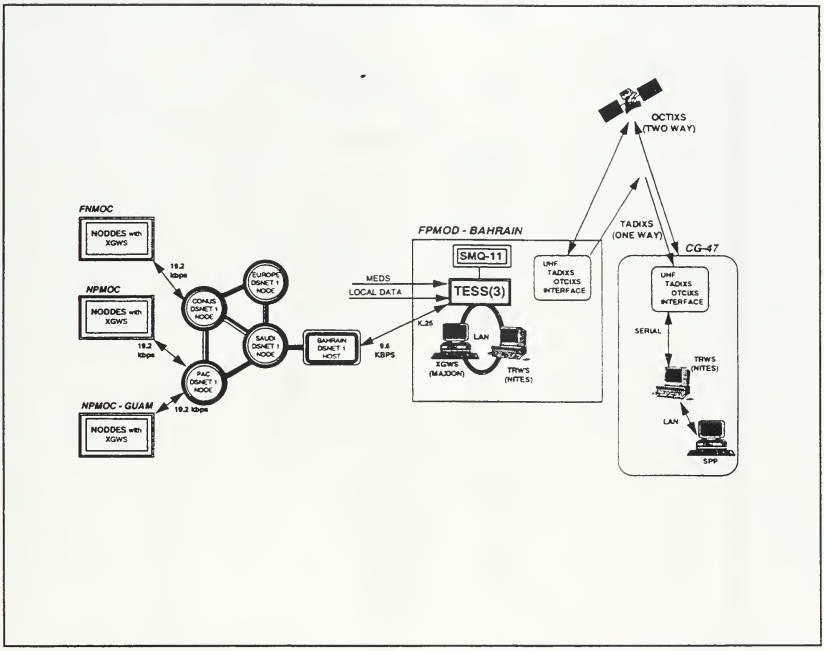

Figure 5.1 Overall data flow and communications connectivity for the EM/EO support system during SHAREM 110 (after Integrated Performance Systems 1994).

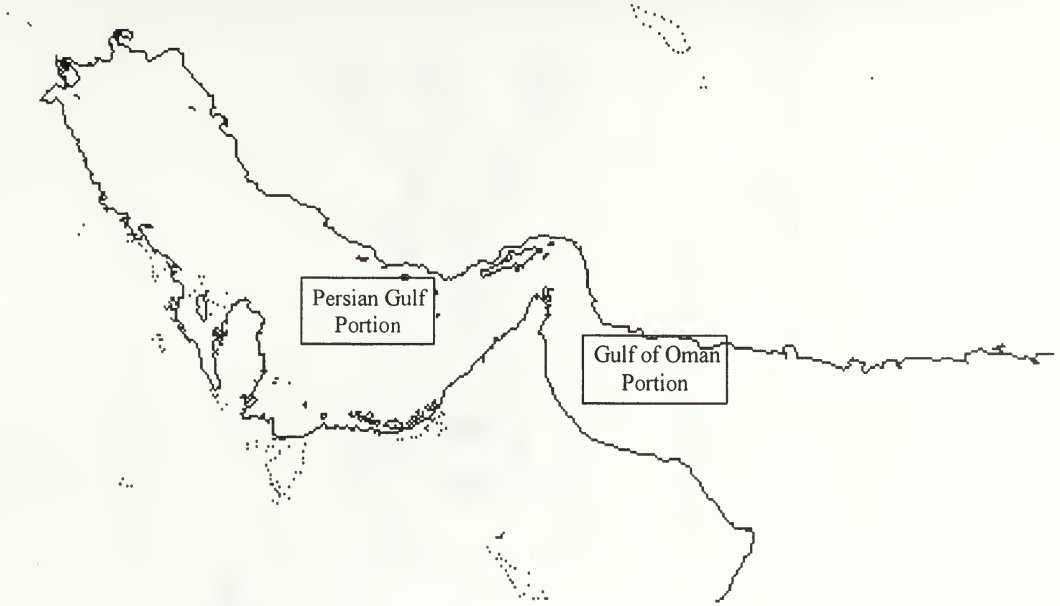

Figure 5.2 Region of data collection and general geography/topography of the Persian Gulf and Gulf of Oman during SHAREM 110.

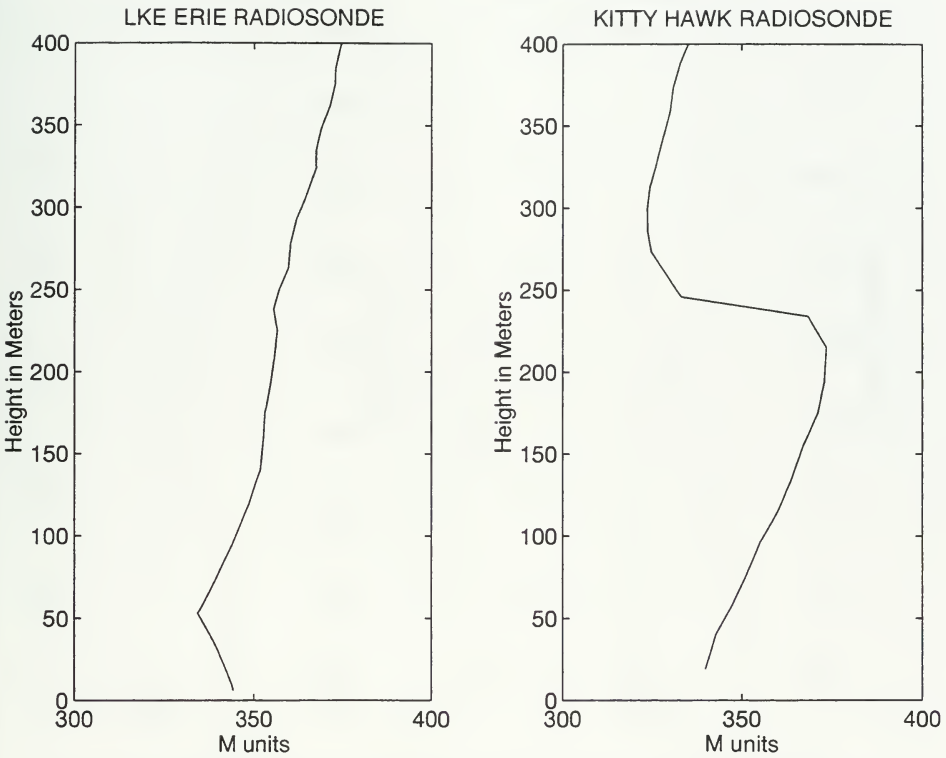

Figure 6.1 Modified refractivity versus altitude profiles for radiosondes launched from the USS Lake Erie and USS Kitty Hawk. Note the lack of data from 10 m to the surface for the USS Lake Erie and 20 m to the surface for the USS Kitty Hawk.

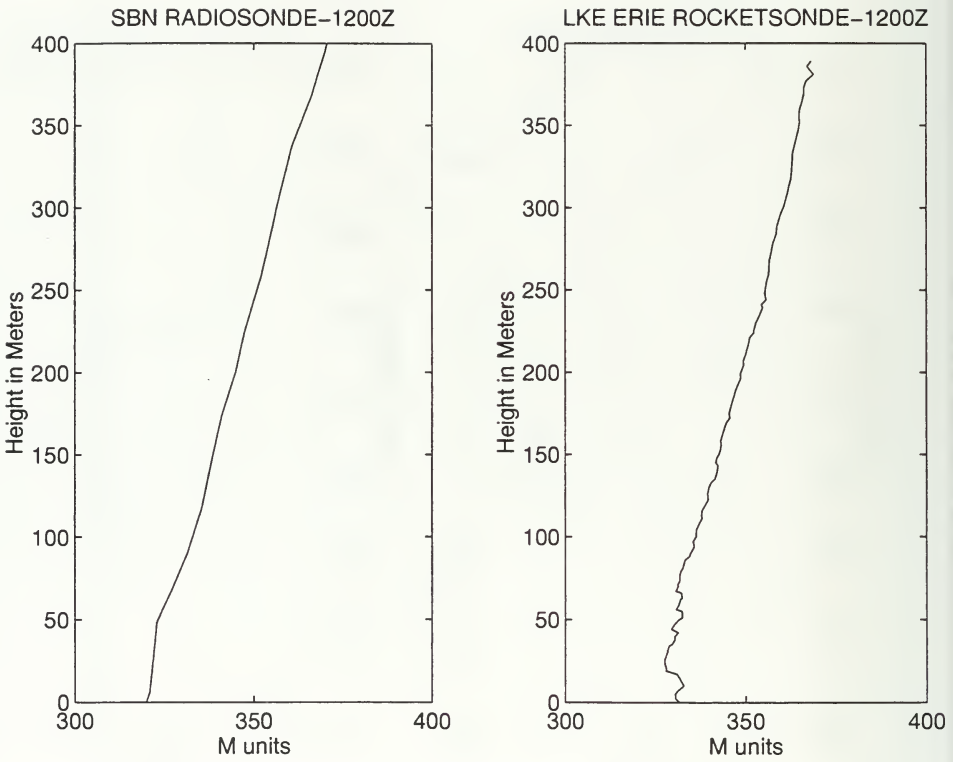

Figures 6.2a & 6.2b Figure 6.2a is the USNS Silas Bent radiosonde launched at 1200Z 11 February 1995 with the gradient between the first two M units extended to the surface. Figure 6.2b is the USS Lake Erie rocketsonde at 1200Z 11 February 1995 with the measured data to the surface.

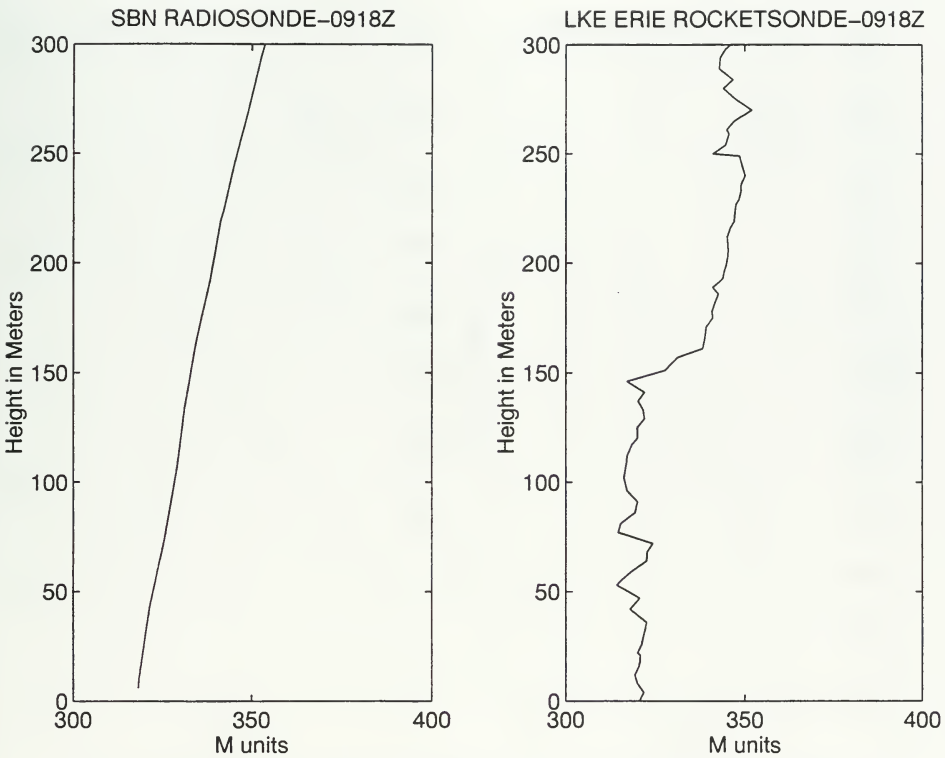

Figure 6.3 M unit versus altitude profiles for radiosonde and rocketsonde soundings taken at 1800Z 09 February 1995.

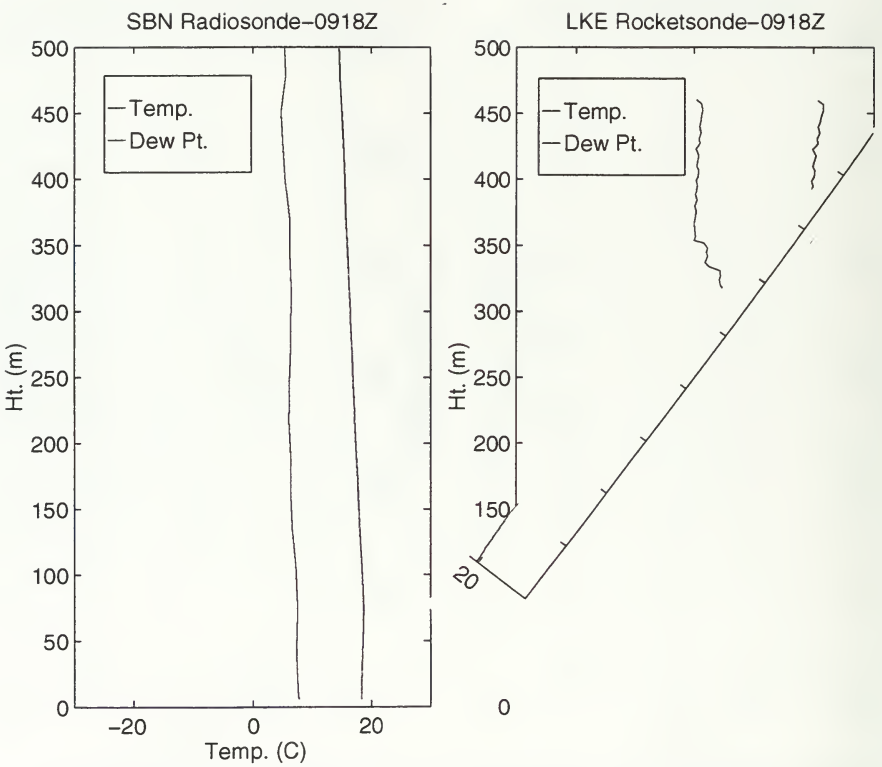

Figure 6.3a Temperature-Dew Point versus altitude profiles for radiosonde and rocketsonde conducted on 1800Z 09 February 1995 during SHAREM 110.

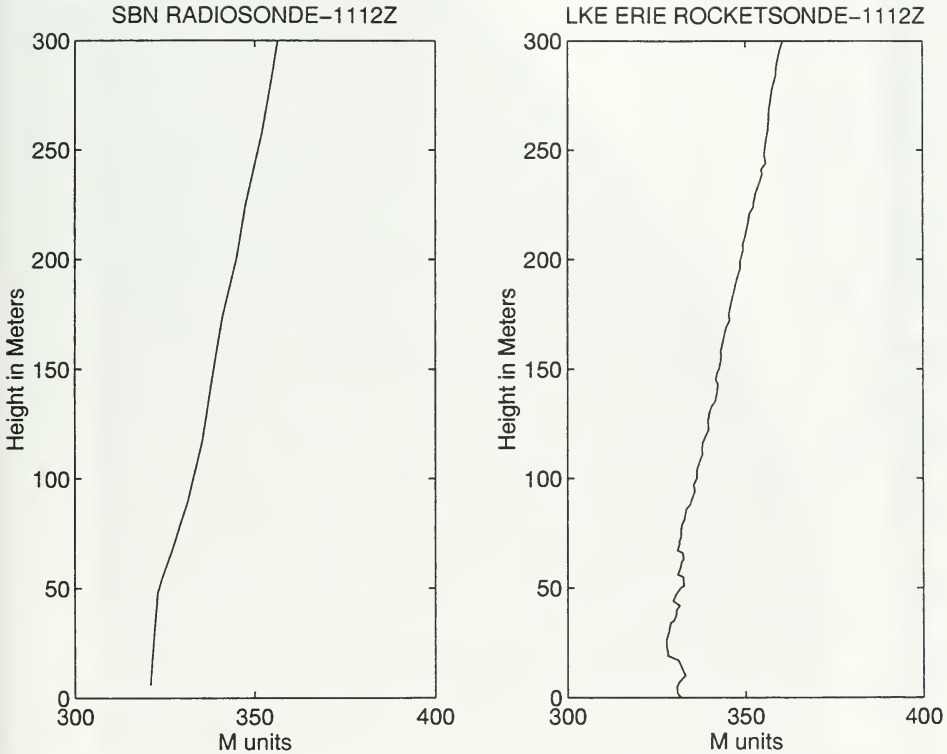

Figure 6.4 M unit versus altitude profiles for radiosonde and rocketsonde profiles conducted on 1200Z 11 February 1995 during SHAREM 110.

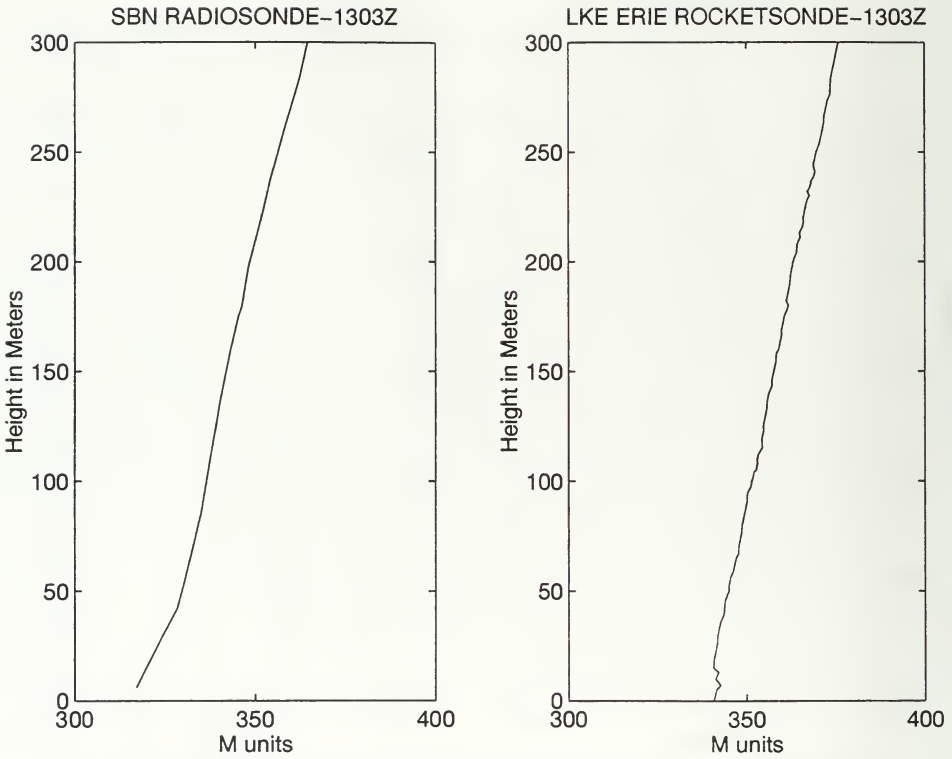

Figure 6.5 M unit versus altitude profiles for radiosonde and rocketsonde soundings conducted on 0300Z 13 February 1995 during SHAREM 110.

Figure 6.6 Propagation loss calculated by RPO version 1.15 for radiosonde launched from USNS Silas Bent 1800Z 09 February 1995 during SHAREM 110.

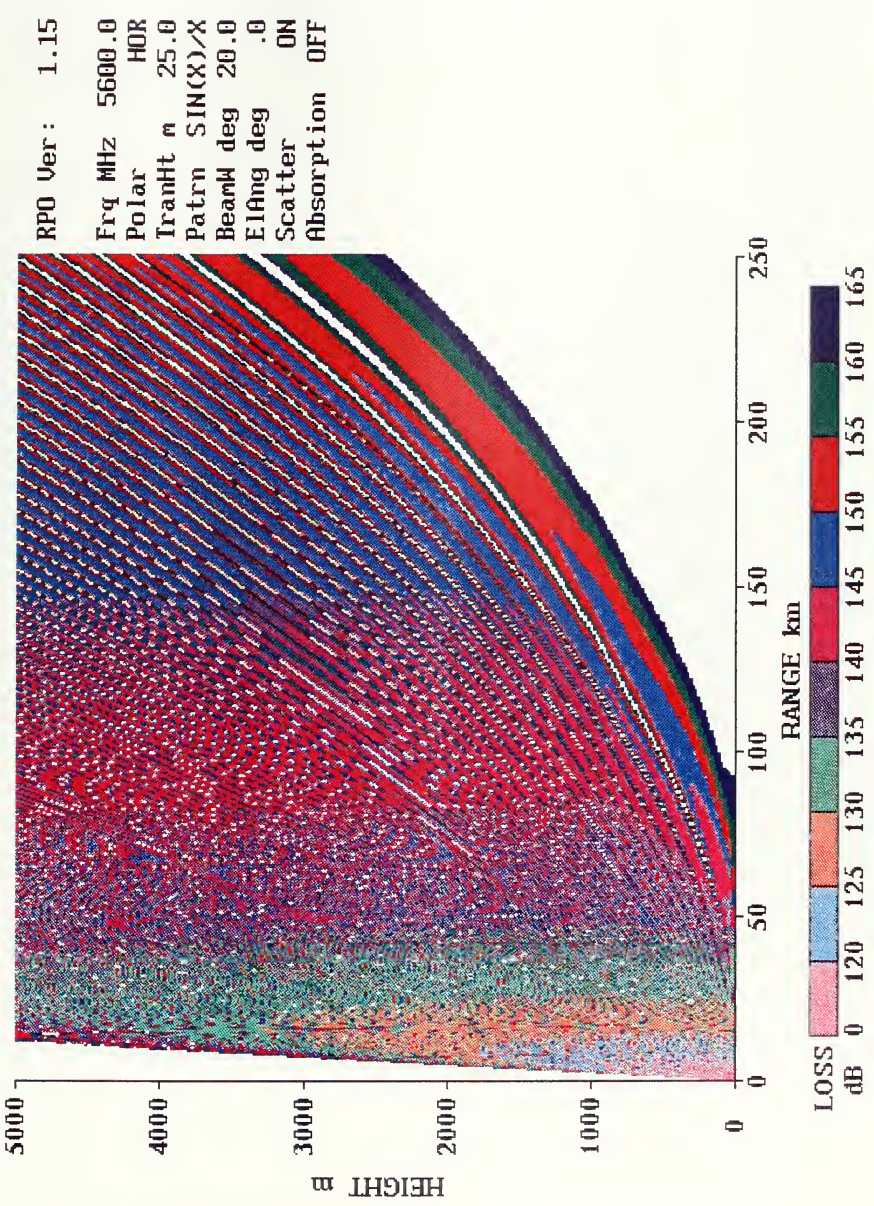

Figure 6.7 Propagation loss calculated by RPO version 1.15 for radiosonde launched from USNS Silas Bent 1200Z 11 February 1995 during SHAREM 110.

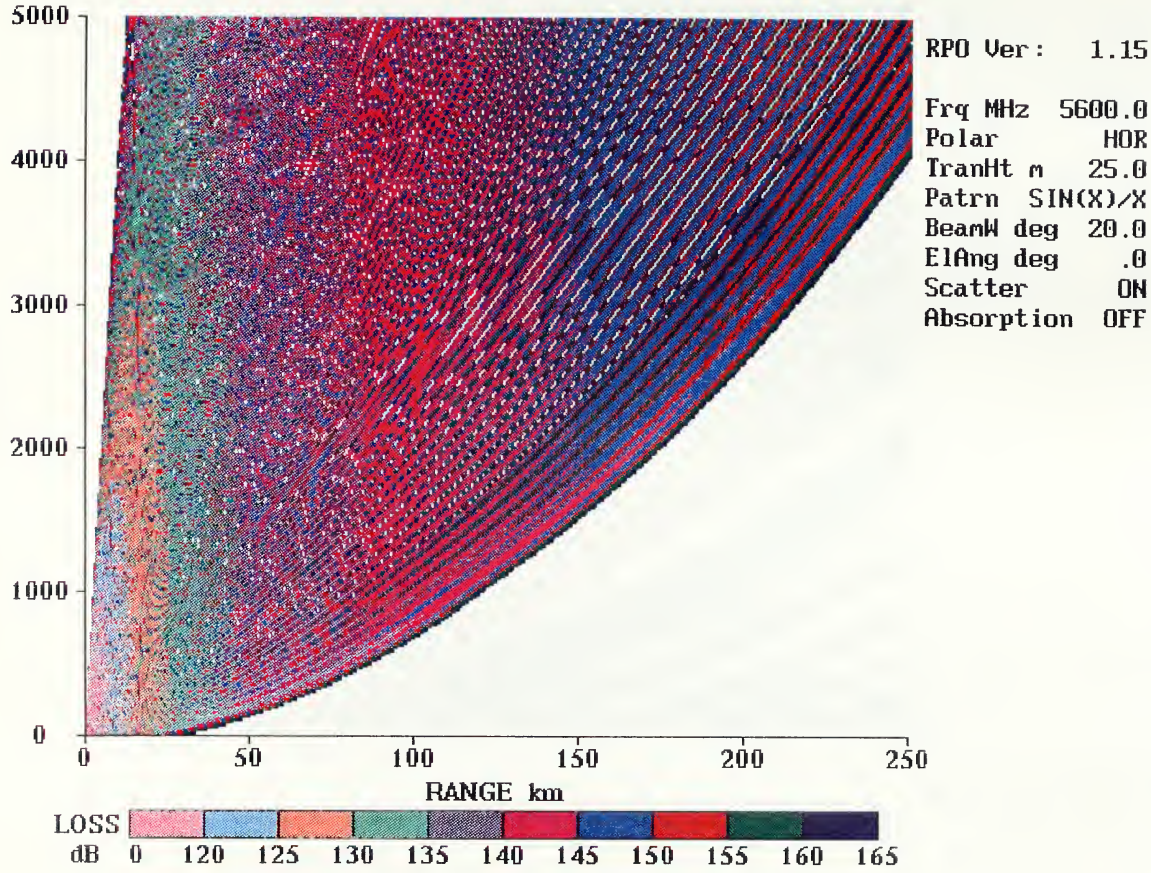

Figure 6.8 Propagation loss calculated by RPO version 1.15 for radiosonde launched from USNS Silas Bent 0300Z 13 February 1995 during SHAREM 110.

Figure 6.9 Propagation loss calculated by RPO version 1.15 for rocketsonde launched from USS Lake Erie 1800Z 09 February 1995 during SHAREM 110.

Figure 6.10 Propagation loss calculated by RPO version 1.15 for rocketsonde launched from USS Lake Erie 1200Z 11 February 1995 during SHAREM 110.

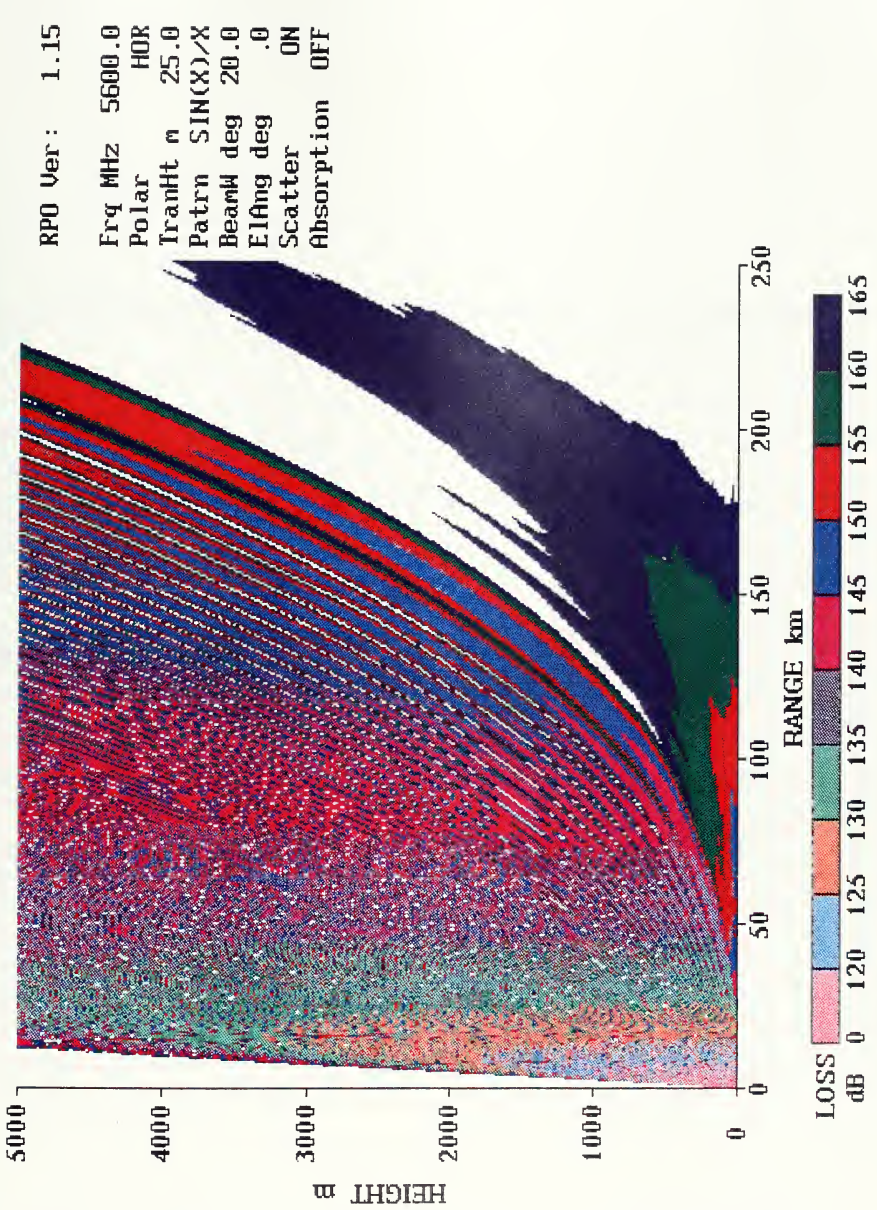

Figure 6.11 Propagation loss calculated by RPO version 1.15 for rocketsonde launched from USS Lake Erie 0300Z 13 February 1995 during SHAREM 110.

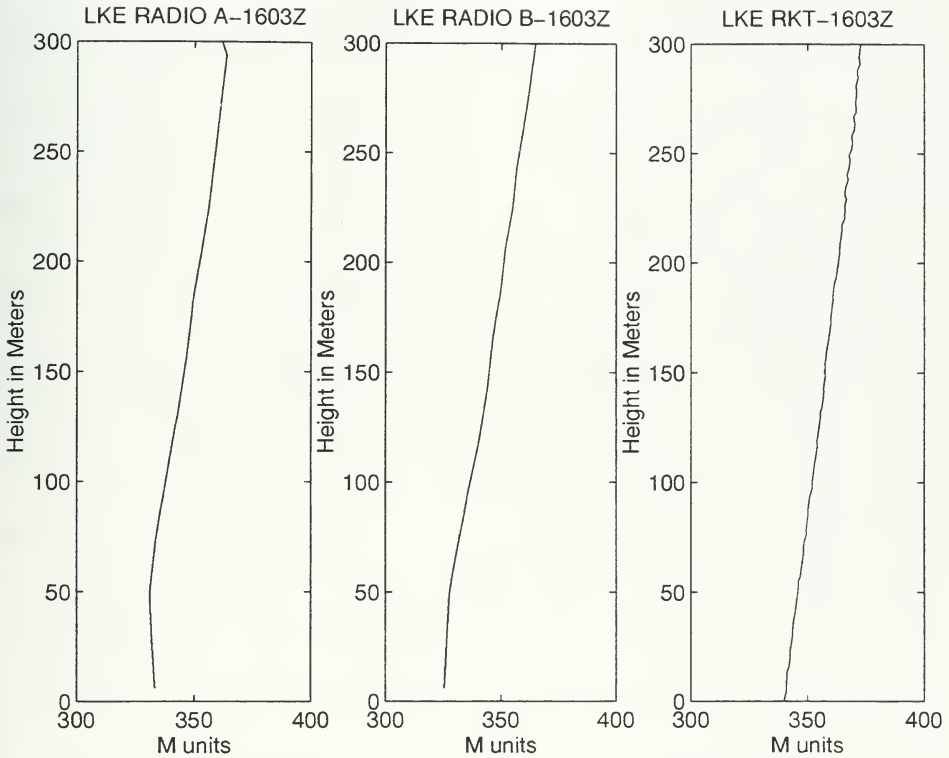

Figure 6.12 M unit versus altitude profiles for radiosonde and rocketsonde soundings conducted 0300Z 16 February 1995 onboard USS Lake Erie during SHAREM 110.

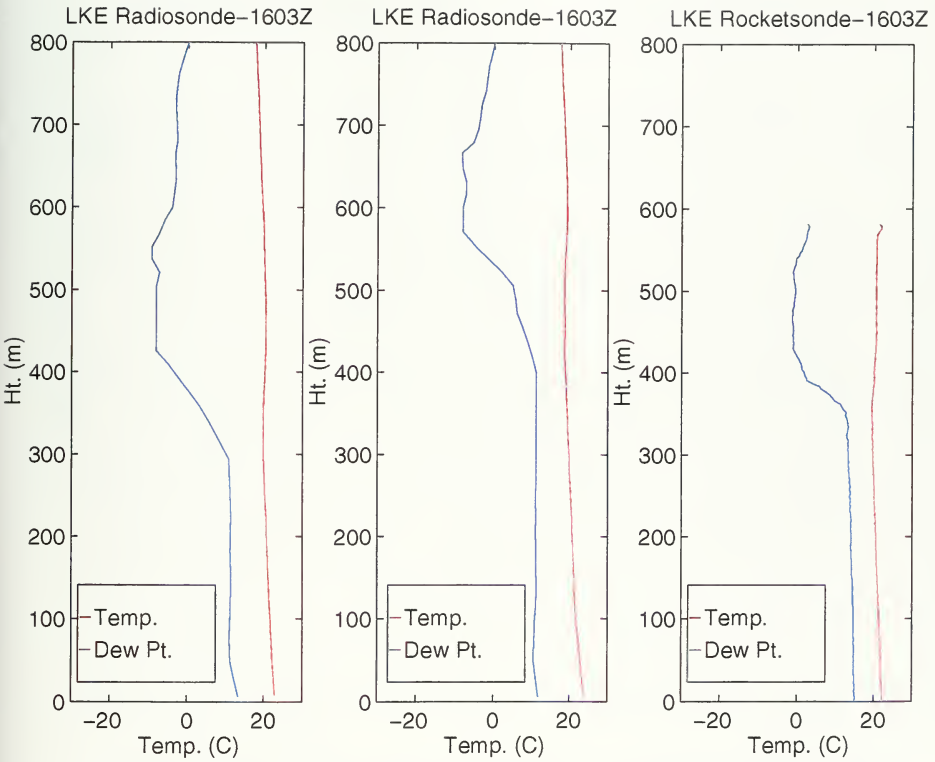

Figure 6.12a Temperature-Dew Point versus altitude profiles for radiosondes and rocketsonde conducted on 0300Z 16 February 1995 during SHAREM 110.

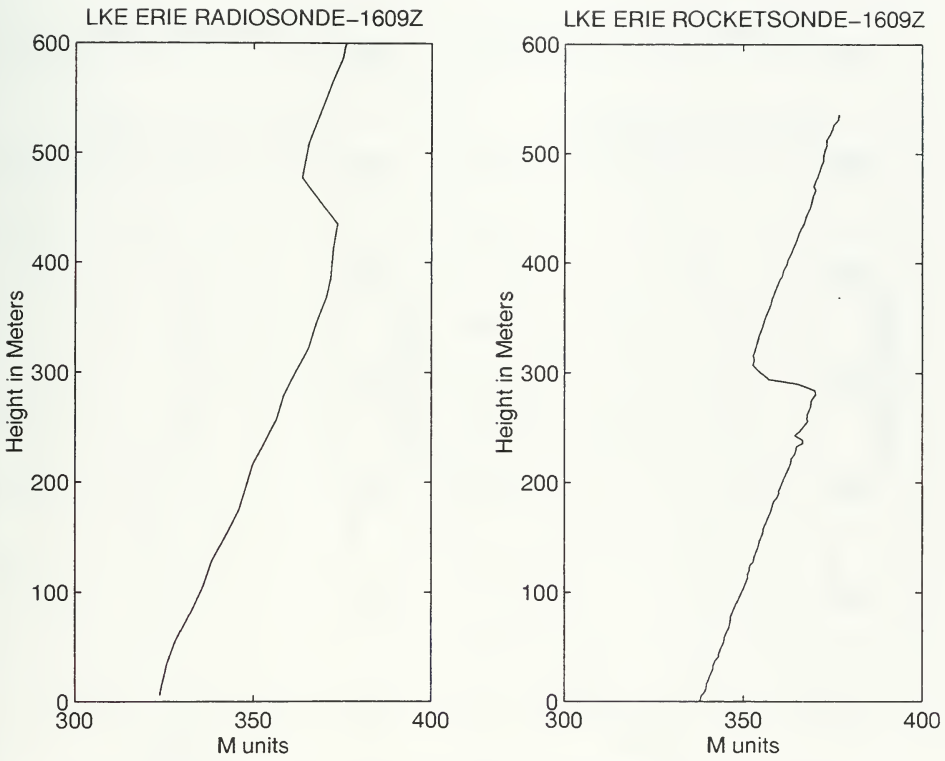

Figure 6.13 M unit versus altitude profiles for radiosonde and rocketsonde soundings conducted 0900Z 16 February 1995 onboard USS Lake Erie during SHAREM 110.

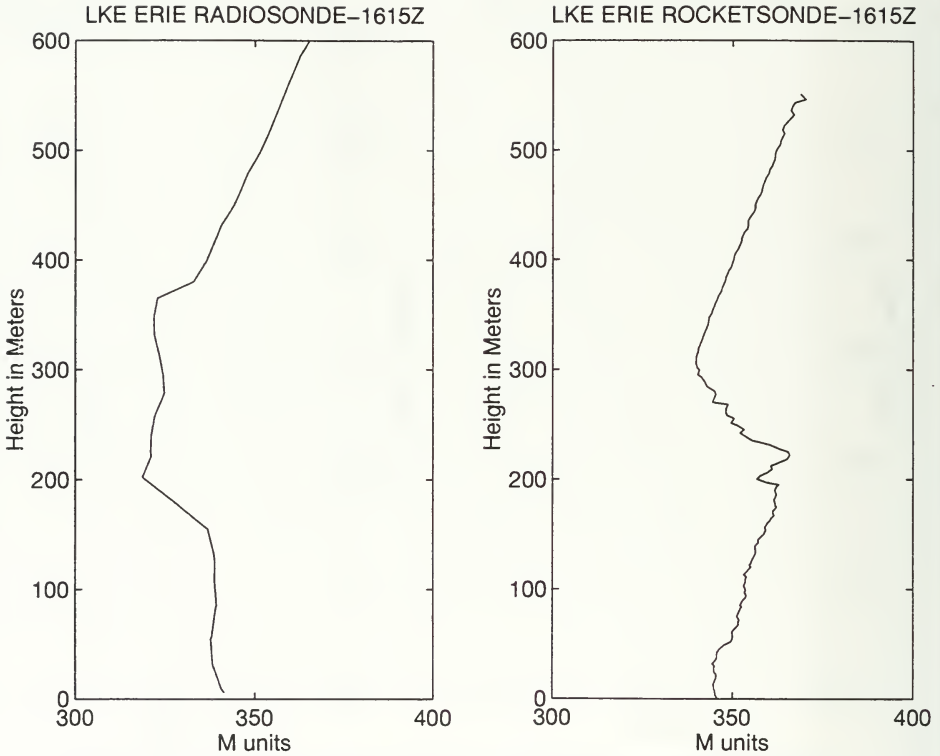

Figure 6.14 M unit versus altitude profiles for radiosonde and rocketsonde soundings conducted 1500Z 16 February 1995 onboard USS Lake Erie during SHAREM 110.

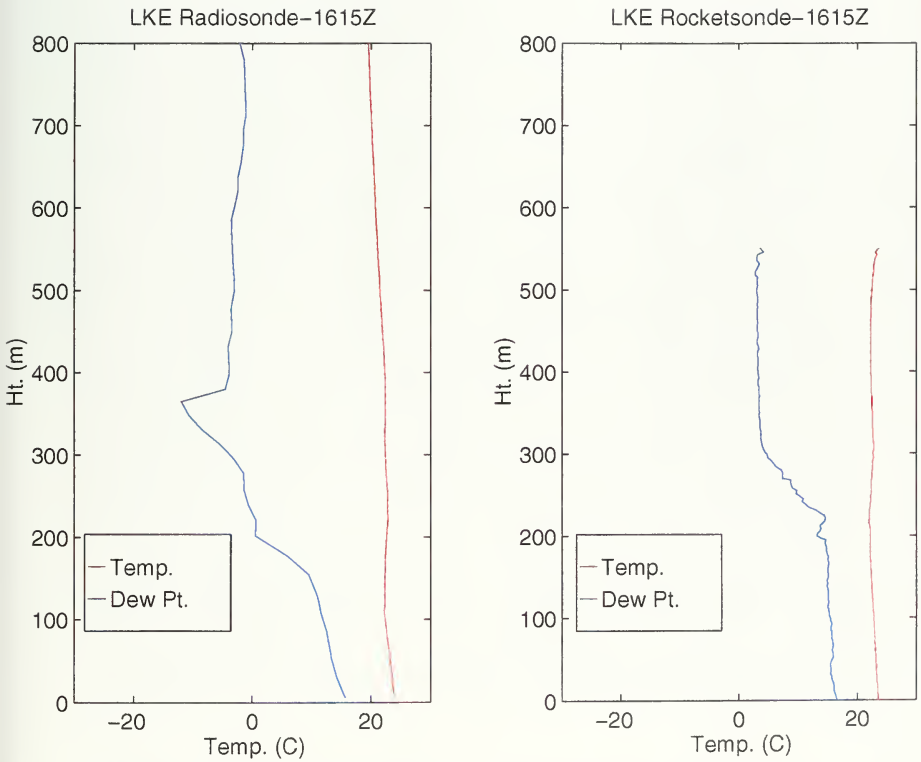

Figure 6.14a Temperature-Dew Point versus altitude profiles for radiosonde and rocketsonde conducted on 1500Z 16 February 1995 during SHAREM 110.

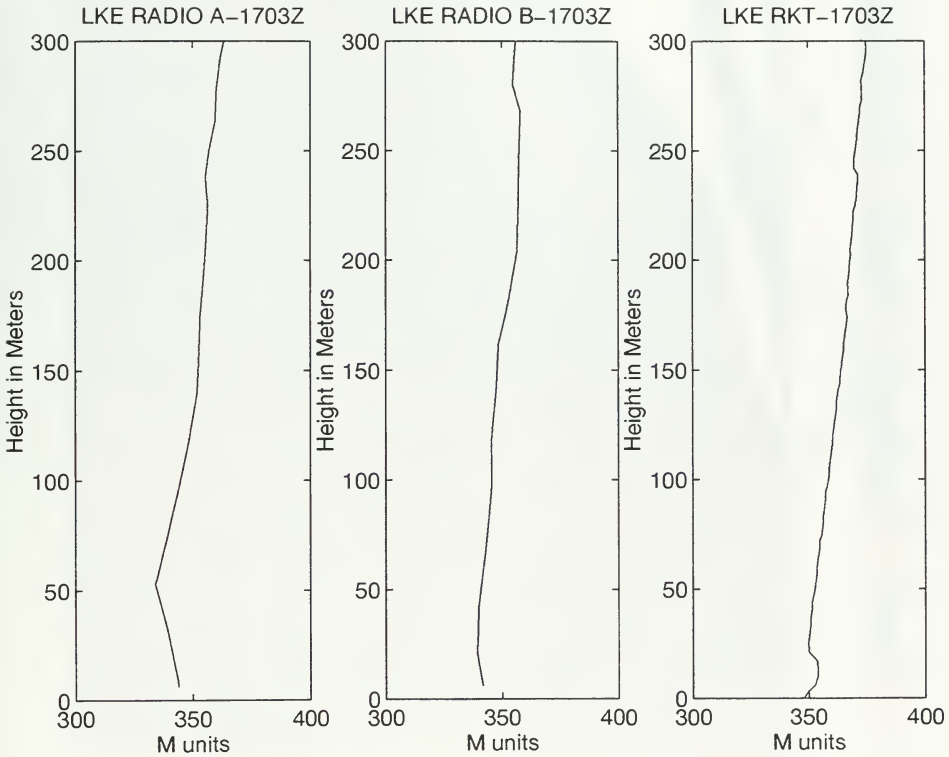

Figure 6.15 M unit versus altitude profiles for radiosonde and rocketsonde soundings conducted 0300Z 17 February 1995 onboard USS Lake Erie during SHAREM 110.

Figure 6.16 Propagation loss calculated by RPO version 1.15 for radiosonde launched from USS Lake Erie 0300Z 16 February 1995 during SHAREM 110.

Figure 6.17 Propagation loss calculated by RPO version 1.15 for radiosonde launched from USS Lake Erie 0300Z 16 February 1995 during SHAREM 110.

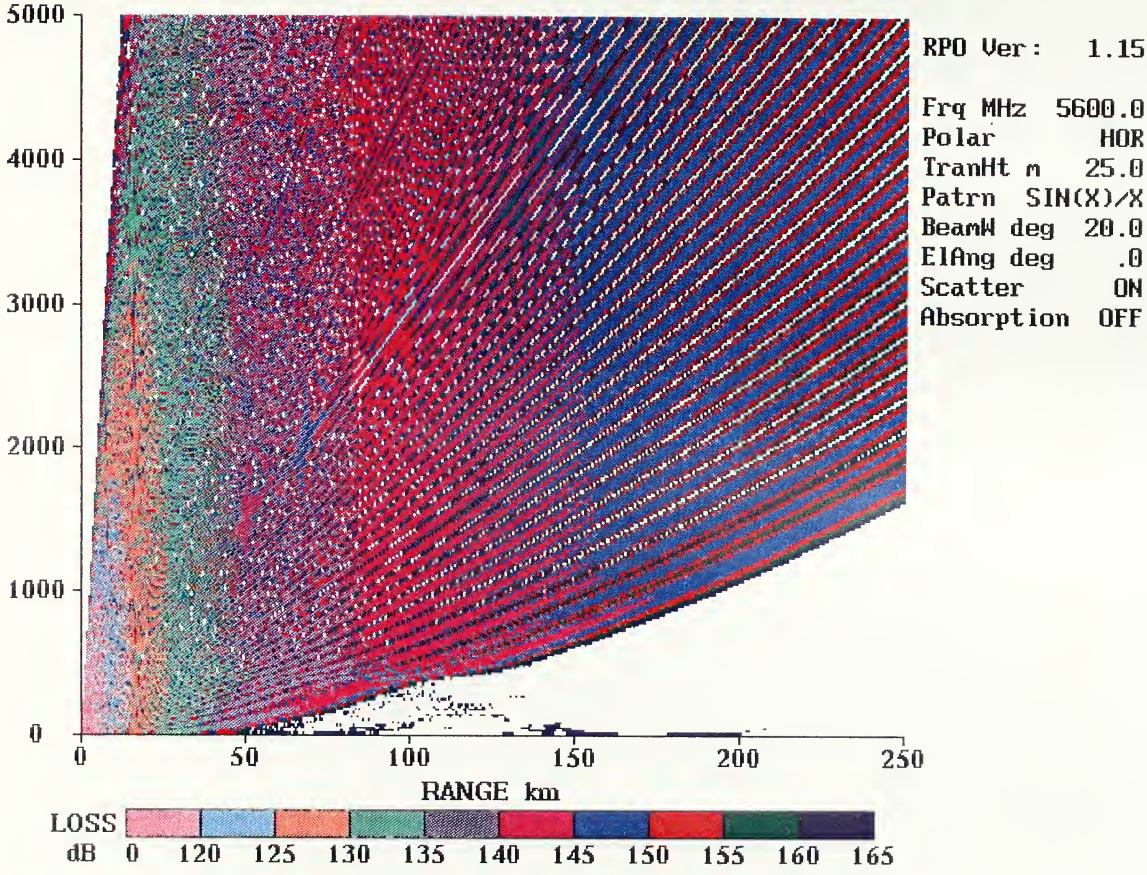

Figure 6.18 Propagation loss calculated by RPO version 1.15 for rocketsonde launched from USS Lake Erie 0300Z 16 February 1995 during SHAREM 110.

Figure 6.19 Propagation loss calculate by RPO version 1.15 for radiosonde launched from USS Lake Erie 0900Z 16 February 1995 during SHAREM 110.

Figure 6.20 Propagation loss calculated by RPO version 1.15 for rocketsonde launched from USS Lake Erie 0900Z 16 February 1995 during SHAREM 110.

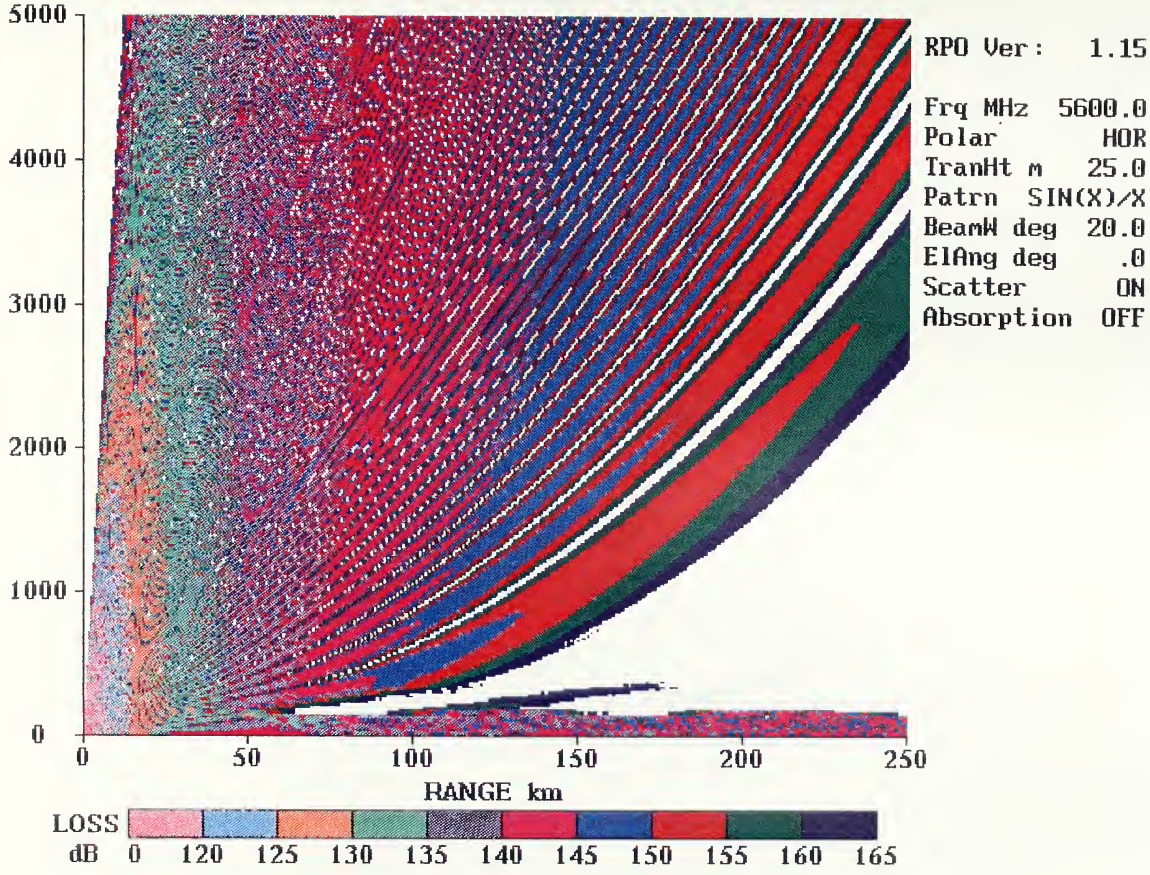

Figure 6.21 Propagation loss calculated by RPO version 1.15 for radiosonde launched from USS Lake Erie 1500Z 16 February 1995 during SHAREM 110.

Figure 6.22 Propagation loss calculated by RPO version 1.15 for rocketsonde launched from USS Lake Erie 1500Z 16 February 1995 during SHAREM 110.

Figure 6.23 Propagation loss calculated by RPO version 1.15 for radiosonde launched from USS Lake Erie 0300Z 17 February 1995 during SHAREM 110.

Figure 6.24 Propagation loss calculated by RPO version 1.15 for radiosonde launched from USS Lake Erie 0300Z 17 February 1995 during SHAREM 110.

Figure 6.25 Propagation loss calculated by RPO version 1.15 for rocketsonde launched from USS Lake Erie 0300Z 17 February 1995 during SHAREM 110.

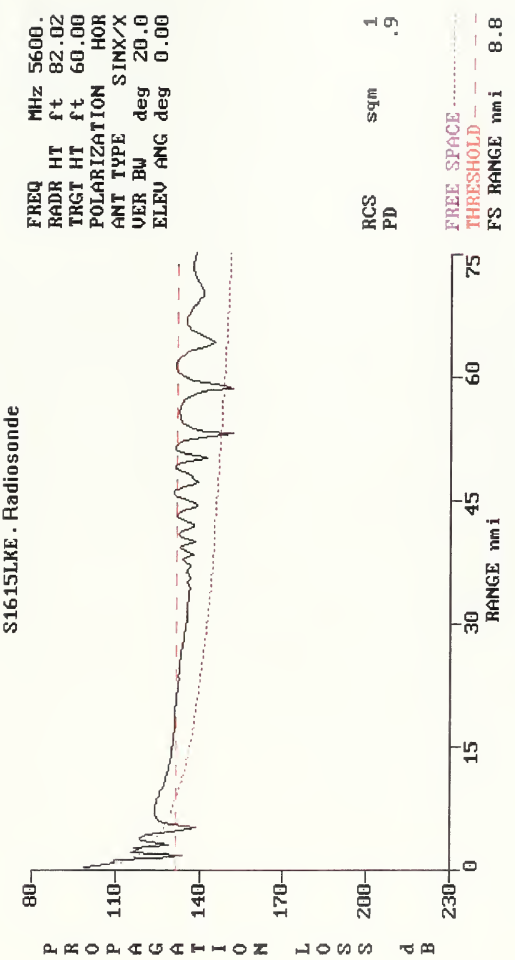

Figure 6.26 Propagation loss versus range calculated by EREPS for radiosonde launched from USS Lake Erie 1500Z 16 February 1995 during SHAREM 110. Threshold of detection based on 1 square m target and 90 percent probability of detection.

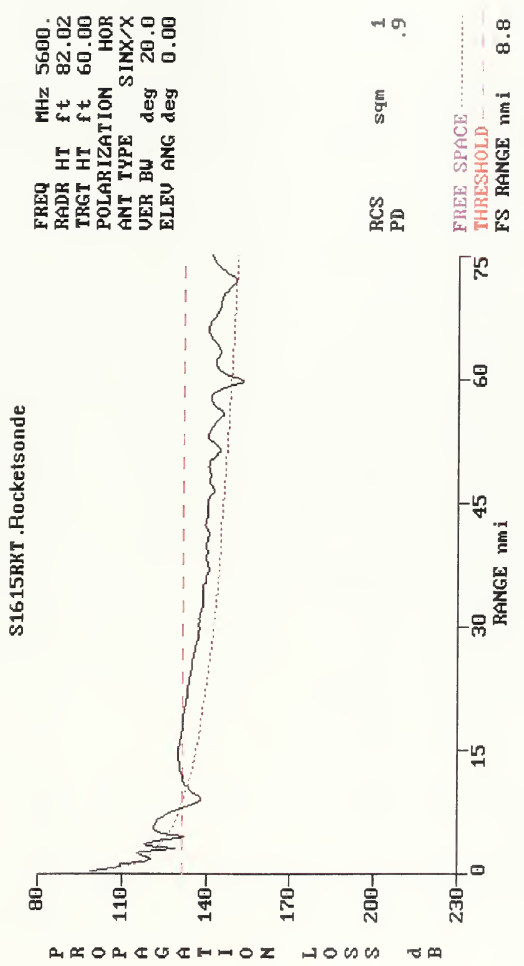

Figure 6.27 Propagation loss versus range calculated by EREPS for rocketsonde launched from USS Lake Erie 1500Z 16 February 1995 during SHAREM 110. Threshold of detection based on 1 square m target and 90 percent probability of detection.

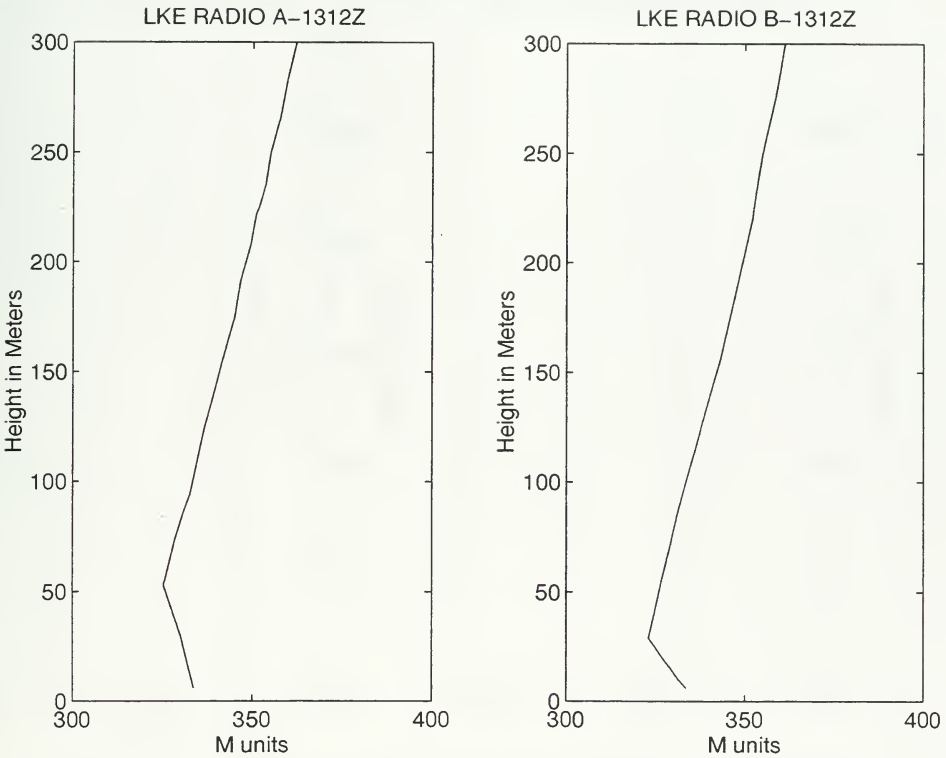

Figure 6.28 M unit versus altitude profiles for two radiosonde soundings launched from USS Lake Erie 1200Z 13 February 1995 during SHAREM 110.

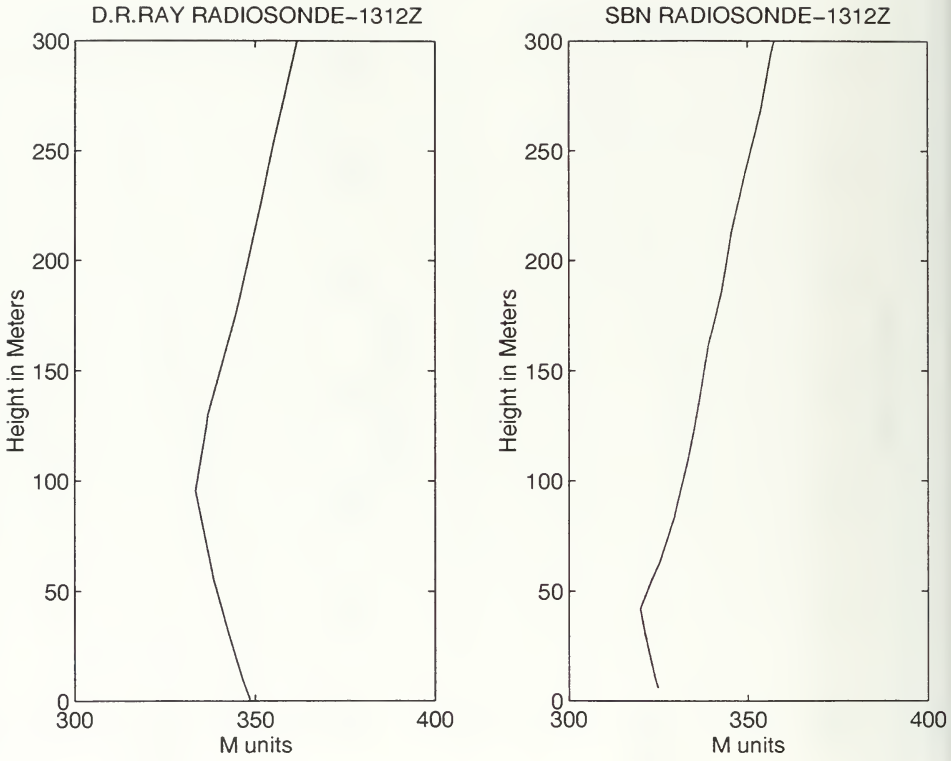

Figure 6.29 M unit versus altitude profiles for radiosonde soundings launched from USS David R. Ray and USNS Silas Bent 1200Z 1300 February 1995 during SHAREM 110.

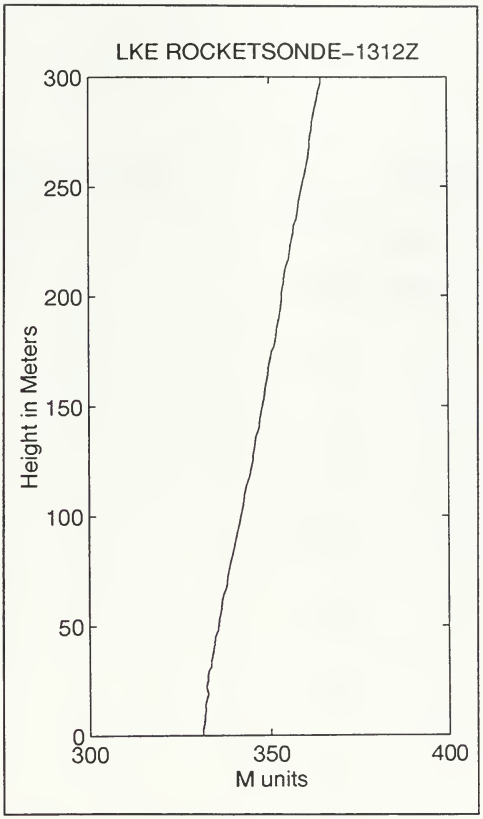

Figure 6.30 M unit versus altitude profile for rocketsonde launched from USS Lake Erie 1200Z 13 February 1995 during SHAREM 110.

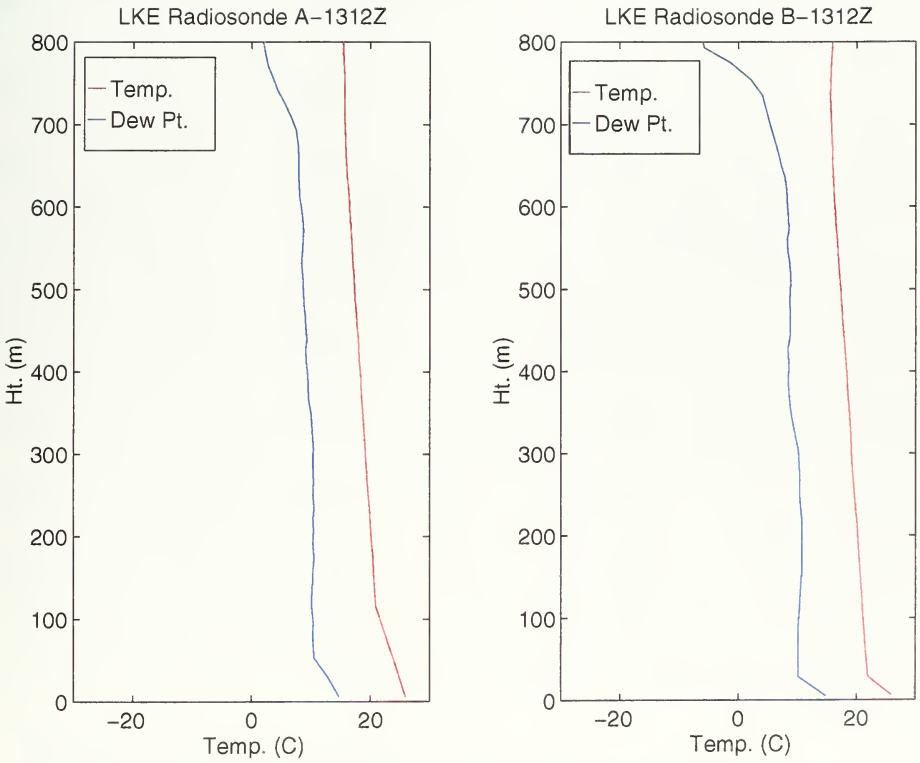

Figure 6.30a Temperature-Dew Point versus altitude profiles for radiosondes conducted on 1200Z 13 February 1995 during SHAREM 110.

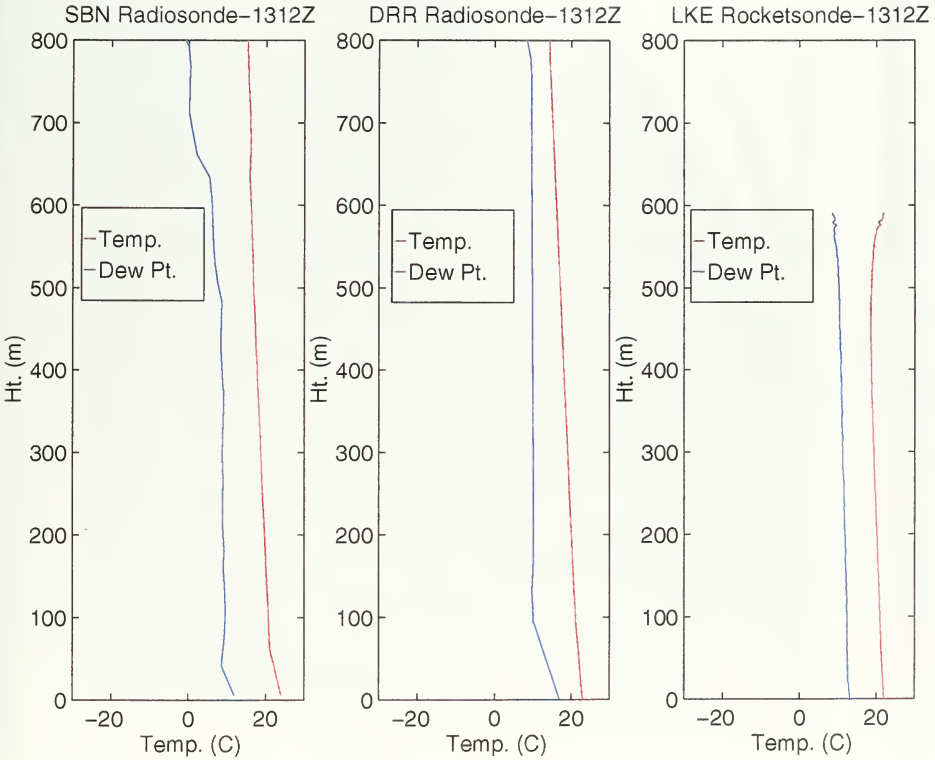

Figure 6.30b Temperature-Dew Point versus altitude profiles for radiosondes and rocketsonde conducted on 1200Z 13 February 1995 during SHAREM 110.

Figure 6.31 Propagation loss calculated by RPO version 1.15 for radiosonde launched from USS Lake Erie 1200Z 13 February 1995 during SHAREM 110.

Figure 6.32 Propagation loss calculated by RPO version 1.15 for radiosonde launched from USS Lake Erie 1200Z 13 February 1995 during SHAREM 110.

Figure 6.33 Propagation loss calculated by RPO version 1.15 for radiosonde launched from USS David R. Ray 1200Z 13 February 1995 during SHAREM 110.

Figure 6.34 Propagation loss calculated by RPO version 1.15 for radiosonde launched from USNS Silas Bent 1200Z 13 February 1995 during SHAREM 110.

Figure 6.35 Propagation loss calculated by RPO version 1.15 for rocketsonde launched from USS Lake Erie 1200Z 13 February 1995 during SHAREM 110.

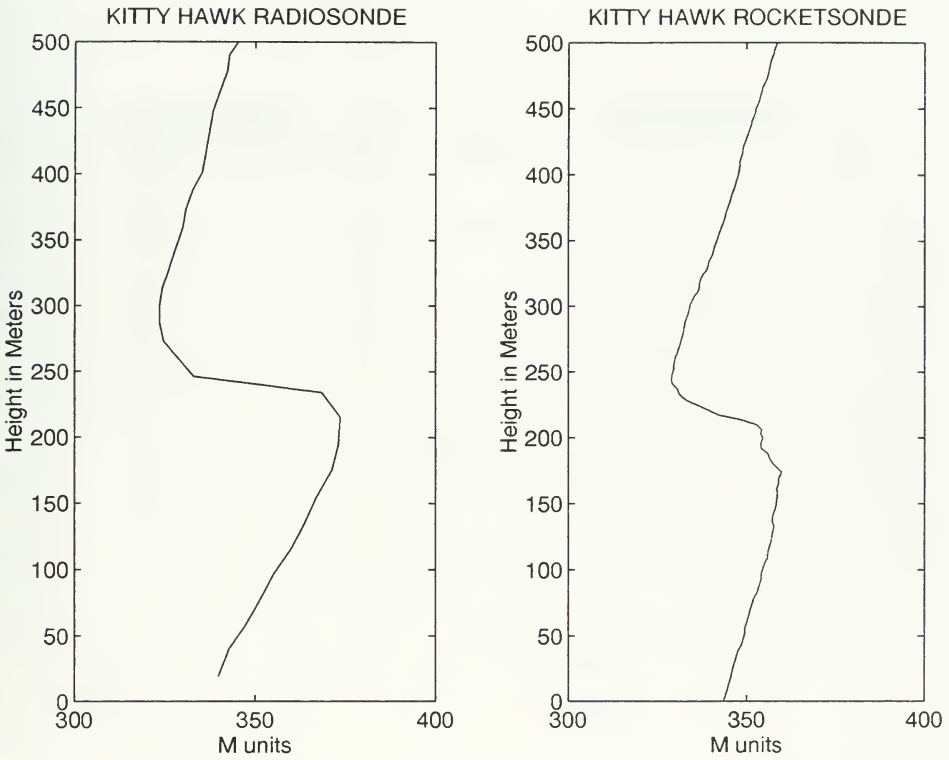

Figure 6.36 M unit versus altitude profiles for simultaneously launched radiosonde and rocketsonde soundings conducted onboard USS Kitty Hawk 21 January 1994

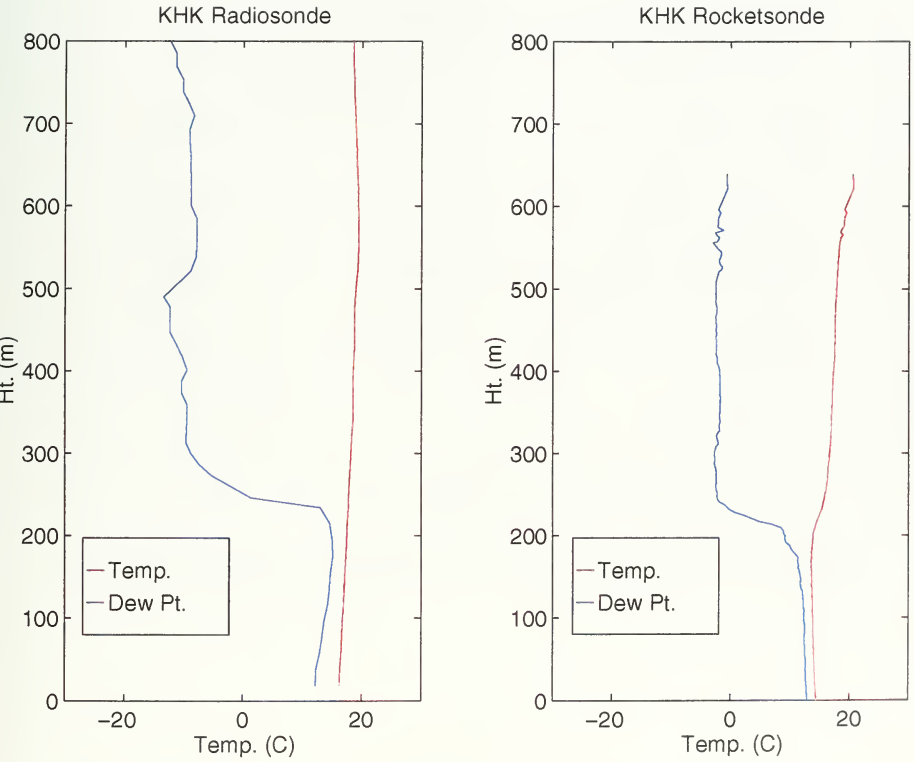

Figure 6.36a Temperature-Dew Point versus altitude profiles for radiosonde and rocketsonde conducted on USS Kitty Hawk 21 January 1994.

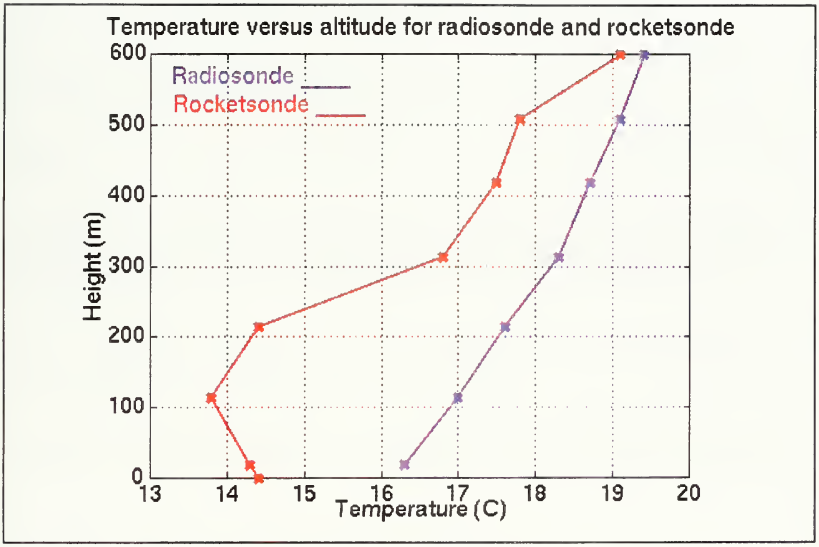

Figure 6.37 Temperature versus altitude for radiosonde and rocketsonde conducted on USS Kitty Hawk 21 January 1994.

LIST OF REFERENCES

Augstein, E., H. Hoeber and Krugermeyer, 1974a: Errors of temperature, humidity, and wind speed measurements on ships in tropical latitudes. *"Meteor" Forschungsergeb. (Berlin)*, Reihe B, No. 9, 1-10.

Blanc, T.V., 1983: A practical approach to flux measurements of long duration in the marine atmospheric surface layer, *J. App. Met.*, **22**, 1093-1110.

Byers, D.J., 1995: Synoptic and mesoscale influences on refraction during SHAREM 110, Master's Thesis, Naval Postgraduate School, Monterey, California, 126 pp.

Call, D.B., 1994: LARDS A low altitude rocket dropsonde with GPS windfinding, Atmospheric Instrumentation Research, Inc., Boulder, Colorado, 12 pp.

Dalton, J.H., 1994: Forward...From the Sea, Library of Congress no. VA 58.4 053 1994, 10 pp.

Dockery, G.D. and Goldhirsh, J., 1994: Atmospheric data resolution requirements for propagation assessment: Case studies of range-dependent coastal environments, *Advisory Group for Aerospace Research and Development Conference Proceedings 567* (AGARD-CP-567), 1-13.

Goerss, J.S. and Duchon, C.E., 1980: Effect of ship heating on dry-bulb temperature measurements in GATE, *J. Phys. Oceanogr.*, **10**, 478-479.

Haney, R.L., 1995: Technical review of the radio physical optics (RPO) model, COMNAVMETOCCOM Independent Model Review Panel (CIMREP) Memorandum, 7 pp.

Helvey, R.A., 1983: Radiosonde errors and spurious surface-based ducts, *IEE Proceedings*, Vol. 130, Part F, No.7, 643-648.

Hoeber, H., 1977: Accuracy of meteorological observations on the ocean. Der Seewart (Hamburg), 38, 204-213.

Integrated Performance Decisions, 1994: SPP-ADM and PMW-175 EM/EO Sharem 110 test plan, Integrated Performance Decisions, Inc., Middletown, RI, 107 pp.

O'Keefe, S., 1992: ...From the Sea-Preparing the Naval service for the 21st Century, Library of Congress no.VA 58.4053 1992, 17 pp.

Patterson, W.L., 1988: Effective use of the electromagnetic products of TESS and IREPS, Naval Ocean Systems Center, Technical Document 1369, 138 pp.

Patterson, W.L. and Hitney, H.V., 1992: Radio physical optic CSCI software documents, Naval Command, Control and Ocean Surveillance Center RDT&E Division, Technical Document 2403, 318 pp.

Program Executive Officer for Undersea Warfare-Advanced Systems Technology Office (PEO USW/ASTO-E), 1995: Input for Sharem 110 quicklook, Surface Warfare Development Group, 10 pp.

Reed, R.K., 1978: An example of shipboard air temperature errors. *Mariners Wea. Log*, **22**, 13-14.

Roll, H.R., 1965: Physics of the marine atmosphere, Academic Press, 426 pp. [Available from Academic Press, Inc., 111 Fifth Avenue, New York, New York 10003].

Rowland, J.R. and Babin, S.M., 1987: Fine-scale measurements of microwave refractivity profiles with helicopter and low-cost rocket probes, Johns Hopkins APL Technical Digest, Vol. 8, No. 4, 5 pp.

INITIAL DISTRIBUTION LIST

		No. Copies
1.	Defense Technical Information Center 8725 John J. Kingman Rd., STE 0944 Ft. Belvoir, VA 22060-6218	2
2.	Dudley Knox Library Naval Postgraduate School 411 Dyer Rd. Monterey, CA 93943-5101	2
3.	Commander Naval Meteorology and Oceanography Command Stennis Space Center, Mississippi 39529-5000	1
4.	Commander Space and Naval Warfare Systems Command (PMW-185) Washington D.C. 20363-5100 Attn: CAPT W. Shutt	1
5.	Commander Space and Naval Warfare Command (PMW-185-3B) METOC Systms Program Office Arlington, VA 22245-5200 Attn: CDR T. Sheridan	1
6.	Chief of Naval Research 800 North Quincy Street Arlington, Virginia 22217	1
7.	Naval Air Warfare Center Weapons Division NAWCWPNS, Geophysics Division Code P3542 Point Mugu, CA 93042-5001 Attn: Roger Helvey	1
8.	Johns Hopkins University Applied Physics Lab Laurel Rd. Laurel, MD 20723-6099 Attn: John Rowland	1

9.	Applied Research Laboratory The Pennsylvania State University P.O. Box 30 State College, PA 16804-0030 Attn: Professor Philbrick	1
10.	Aegis Program Manager PMS 400 B30AD Arlington, VA 22242-5186 Attn: LCDR Robert Dees	1
11.	Naval Research Laboratory, TOWS Stennis Space Center, Mississippi 39529-4004 Attn: Ken Ferer/E. Mozley	1
12.	Oceanographer of the Navy Naval Observatory 34th and Massachusetts Avenue NW Washington DC 20390-5000 Attn: Franceen George	1
13.	METOC Technology Division Planning Systems Incorporated 7923 Jones Branch Drive McLean, VA 22102 Attn: Rick Hillyer	1
14.	Naval Research Laboratory Naval Postgraduate School Annex Monterey, California 93940-5006 Attn: A. Goroch/J. Cook	1
15.	Professor K. Davidson Meteorology Department, Code MR/DS Naval Postgraduate School Monterey, California 93943-5002	3
16.	Professor C. Wash Meteorology Department, Code MR/WX Naval Postgraduate School Monterey, California 93943-5002	2

17. LCDR Brian K. Baldauf, USN 1
U.S. Naval Forces Korea
Unit 15250
APO AP 96205-0023